"In presenting the dissertation as a partial fulfillment of the requirements for an advanced degree from the Georgia Institute of Technology, I agree that the Library of the Institution shall make it available for inspection and circulation in accordance with its regulations governing materials of this type. I agree that permission to copy from, or to publish from, this dissertation may be granted by the professor under whose direction it was written, or, in his absence, by the dean of the Graduate Division when such copying or publication is solely for scholarly purposes and does not involve potential financial gain. It is understood that any copying from, or publication of, this dissertation which involves potential financial gain will not be allowed without written permission.

"

THE NORMAL COMPONENT OF INDUCED VELOCITY FOR A LIFTING ROTOR IN GROUND EFFECT

A THESIS

Presented to the

Faculty of the Graduate Division

by

James Lyons Tow

In Partial Fulfillment

of the Requirements for the Degree

Master of Science in Aeronautical Engineering

Georgia Institute of Technology

May, 1962

THE NORMAL COMPONENT OF INDUCED VELOCITY FOR

A LIFTING ROTOR IN GROUND EFFECT

Approved:

... Castles, Jr.

Robin B. Gray

Thomas W. Jackson

Date approved by Chairman: May 25, 1962

ACKNOWLEDGEMENTS

The author wishes to express his appreciation to Professor Walter Castles, Jr., for the suggestion of the topic and for his valuable guidance throughout the conduct of this study. Gratitude is also extended to Doctor Robin B. Gray and Doctor Thomas W. Jackson for their review and comments on the material contained herein.

TABLE OF CONTENTS

LIST OF TABLES

LIST OF FIGURES

LIST OF SYMBOLS

C_T	Rotor thrust coefficient, $T/\rho \pi \Omega^2 R^4$
P_i	Induced power required, in ground effect
R	Radius of the rotor
R_v	Radius of the vortex cylinder
T	Rotor thrust
V	Velocity of helicopter along flight path
V_i	Normal component of velocity induced at a point P
$V_{i\ mean}$	Mean value of distribution of normal component of induced velocity along longitudinal diameter of rotor, equal to $V_{i\ center}$ for uniformly loaded rotor out of ground effect
$V_{i\ center}$	Value of normal component of induced velocity at the center of a rotor, equal to $V_{i\ mean}$ for a uniformly loaded rotor out of ground effect
$V_{i\ ref}$	Reference, or average, value of the normal component of induced velocity for the case of triangular loading
ΔV_i	Interference velocity due to presence of ground, positive upward
v	Normal component of induced velocity at the center of a rotor. For uniformly loaded rotor out of ground effect, equals $V_{i\ center}$ and $V_{i\ mean}$.
X, Y, Z	Rotor axes
α	Angle of attack of the rotor tip-path plane
Γ	Vortex strength
λ	$V(\sin \alpha - v)/\Omega R$
μ	$V \cos \alpha/\Omega R$

ρ	Density of air
χ	Wake angle, angle between the axis of the wake and the normal to the tip-path plane

Subscripts:

center	Reference to center of rotor
IGE	In ground effect
mean	Mean value or based on mean values
OGE	Out of ground effect
$\chi=0$	Wake angle of zero degrees, hovering rotor

SUMMARY

The distributions of the normal component of induced velocity were determined along the longitudinal diameter of lifting rotors in ground effect. The induced velocity distributions were calculated for rotor heights above the ground plane of 0.5, 0.6, 0.8, and 1.0 radii, and for wake angles of 0, 14.04, 26.56, 45.00, and 63.43 degrees.

This analysis is based on the method of reflection wherein the ground effect is simulated by a mirror image of the rotor vortex system, which exists above the ground plane, for a rotor operating at a given height and wake angle. Use was made of existing data dealing with the normal component of induced velocity for a lifting rotor out of ground effect, with consideration being given to assumed load distributions of both the uniform and the triangular type. The results are presented in the form of tables and graphs for the rotor heights considered and for several wake angles in the lower half of the helicopter speed range.

An approximate method is given for the determination of the wake angle and induced power required for a helicopter rotor operating in ground effect.

The results of this study are compared with the limited data available on the subject. The comparisons indicate that the induced velocity at the center point of a rotor does not appear to be representative of the mean value over the rotor as was assumed in NASA TN D-234, and that such an assumption would tend to introduce error into any estimate of the effect of the ground plane.

This analysis indicates that, for lifting rotors, ground effect decreases with increases in either height above the ground or forward speed. The decrease with height above the ground in forward flight is more rapid than that in hovering flight. The rapid decrease of ground effect in forward flight at the lower rotor heights occurs, in part, in the initial portion of the speed range. As a result the mean induced velocity over the rotor increases slightly rather than decreases as the helicopter increases speed.

The induced velocity distributions along the longitudinal diameter of rotors operating in ground effect and having a triangular loading were found to be similar to the distributions for rotors out of ground effect, except that a reduction in the magnitude of the induced velocities occurred with each reduction of rotor height above the ground.

CHAPTER I

INTRODUCTION

The performance of a lifting rotor is directly related to the induced velocities that exist in the vicinity of the rotor. These velocities induced by the rotor vortex system have components in the normal, radial, and rotational directions, but the normal component has by far the largest influence on rotor performance. Thus, to simplify the analysis of the forces acting on lifting rotors, the normal component of induced velocity is frequently the only component considered. Such will be the case in this investigation.

The average induced velocity associated with a required amount of thrust is reduced by the presence of a ground plane, thereby reducing the power required. Heyson (1)* calculated the induced velocity at the center of a lifting rotor under conditions of uniform loading for various combinations of wake angles and rotor heights above the ground plane. It was assumed that the induced velocity at the center of a rotor is proportional to the average induced velocity over the rotor disk. Although the value of induced velocity at the center of a rotor is equal to the average value for a rotor with uniform loading operating out of ground effect, it is uncertain how much error is involved in making Heyson's approximation that the value of induced velocity at the

---

*Numbers in parentheses refer to items in the Bibliography.

center of the rotor is proportional to the average value over the rotor disk when in ground effect. Furthermore, for a rotor with non-uniform loading, there is no particular point on the rotor disk for which the induced velocity has a fixed relation to the average value. Thus, in the present paper, it is proposed that the more accurate approximation be made that the average of the induced velocities over the disk can be taken to be the average value of the induced velocity over the longitudinal axis of the rotor disk.

The flight conditions in which a lifting rotor is most likely to be influenced by the presence of the ground could be related to a helicopter during the execution of a take-off or landing. The scope of this investigation is limited to rotors operating from one-half to one rotor radius above the ground, and to essentially the lower half of the helicopter speed range. In particular, it is the purpose of this study to determine the distribution of the normal component of induced velocity along the longitudinal axis in the plane of a lifting rotor while operating as previously described. Comparison of the results obtained will be made with those presented in reference (1). In addition, some results are given for a rotor assumed to have triangular loading.

This analysis is based on the method of reflection, wherein the ground effect is simulated by a mirror image of the rotor vortex system existing above the ground for a rotor at a given height and wake angle. With this method, the distribution of the normal component of induced velocity was determined for cases of uniform disk loading and triangular disk loading. Data used in this investigation, for the two disk loadings mentioned, were obtained from work done by Castles and De Leeuw (2) and by Heyson and Katzoff (3). In the above reports the normal component of induced velocity of a rotor out of ground effect was presented for disk loadings that were uniform and triangular respectively. For each of the disk loadings considered, the distribution of the normal component of the induced velocity over the rotor has been determined for nondimensional rotor heights of 0.5, 0.6, 0.8, and 1.0; and for rotors operating at wake angles of from 0 to 63.43 degrees. The results obtained in this investigation are presented in both tabular and graphic form. A check on the accuracy of the results of the numerical methods used in the present report was afforded by a comparison with the results obtained by Knight and Hefner (4). The results obtained in this paper were converted to nondimensional ratios which have been compared graphically to those obtained by Heyson in reference (1).

An approximate method for the determination of the wake angle and induced power required for a helicopter in ground effect is included in this paper to illustrate an application of the basic data contained herein.

CHAPTER II

PROCEDURE

Prior to making a study of ground effect on the normal component of induced velocity of a rotor operating at various wake angles, it is necessary to assume a disk load distribution on that rotor. Considerable work has been done in the field of the induced velocities of lifting rotors, and generally, the assumed disk load distributions are either uniform or triangular as shown in Figure 1. Inasmuch as similar information was available for each of the above type loadings, this study considers them both. The primary data used in this analysis are based upon the results presented by Castles and De Leeuw (2) and by Heyson and Katzoff (3), both of which dealt with the normal component of induced velocity in the vicinity of a lifting rotor out of ground effect. A uniform disk loading was assumed by Castles and De Leeuw, whereas Heyson and Katzoff considered a triangular disk loading. In that this study of ground effect on a lifting rotor is based on the data as presented in the reports mentioned above, a general description of their contents is believed to be pertinent to this development.

In consideration of a disk that was uniformly loaded, Castles and De Leeuw assumed the wake vortex distribution of the rotor consisted of a straight elliptic cylinder which was formed by an infinite number of vortex rings of infinitesimal strength, each of which is parallel to the tip path plane of the rotor (Figure 2).

It was shown that such a vortex distribution is equivalent to a single vortex sheet of uniform finite strength per unit length, $\frac{d\Gamma}{dZ}$, measured in the Z direction. Such a vortex sheet forms an elliptic cylinder which coincides with the wake boundary, and its strength can be represented as

$$\frac{d\Gamma}{dZ} = \frac{RC_T \Omega}{(1 - \frac{3}{2}\mu^2)}$$

The component of induced velocity at any point in the vicinity of the rotor can be found by integration of the Biot-Savart integral for the wake vortex system.

The results in reference (2) are presented graphically where lines of constant induced velocity ratio, $\frac{V_i}{V_{i_{mean}}}$, are plotted with coordinates of nondimensional height of the point above or below the rotor plane, $\frac{Z}{R}$, versus nondimensional radius, $\frac{X}{R}$. Values in the longitudinal plane of symmetry are given for the vicinity of a lifting rotor which is operating out of ground effect, and at various wake angles, χ, of from zero to in excess of ninety degrees. The angle, χ, is defined by

$$\chi = \text{Tan}^{-1} \left(\frac{-\mu}{\lambda}\right),$$

as shown in Figure 3.

From the standpoint of uniform loading the data used in this paper in the determination of ground effect are based on the graphs as presented in reference (2), an example of which has been extracted and is given as Figure 4.

The results obtained by Heyson and Katzoff were used in this paper when consideration was given to the condition of triangular disk loading. In the development by Heyson and Katzoff, the assumed condition of non-uniform disk loading was represented by a distribution of shed vortex cylinders (Figure 2), all of which are parallel and concentric. The contribution of any single vortex cylinder was determined from the graphs of reference (2), and then the total induced flow at the point $\frac{X}{R}$, $\frac{Y}{R}$, $\frac{Z}{R}$ was read directly from the graphs of reference (2) at the point $(\frac{X}{R})(\frac{R}{R_v})$, $(\frac{Y}{R})(\frac{R}{R_v})$, $(\frac{Z}{R})(\frac{R}{R_v})$, where R_v is the radius of the vortex cylinder, and R is the rotor radius. Thus, having assumed a finite number of superimposed concentric vortex cylinders of suitable strength and dimensions, the induced velocity at a given point, and hence, throughout the flow field of a non-uniformly loaded rotor, was determined by adding the values of induced velocity, as induced by each of the vortex cylinders comprising the wake, with consideration given to the positive or negative influence each vortex cylinder has in the composite system. The results in reference (3) are presented in a manner similar to those in reference (2) in that lines of constant induced velocity ratio, $\frac{V_i}{V_{i\ ref}}$, are shown for the vicinity of a lifting rotor operating at various wake angles. An example of such a graph is shown by Figure 5.

The rotor wake configuration used in this analysis is one in which a mirror image of the vortex system existing above the ground is used to provide the equivalence of the ground effect. A separate rotor wake configuration was used for each rotor height and wake angle combination. A representation of the wake of a rotor in the presence of the ground as used in this paper is as shown in Figure 6.

Considering first a uniformly loaded rotor, the first data used in the present investigation was that presented in reference (2), or specifically, that given by the graphs of the induced velocity ratio, $\frac{V_i}{V_{i_{mean}}}$, for the vicinity of a lifting rotor which was operating with wakes at various angles.

As an example, the rotor shown operating with a wake angle of $\chi = 45°$ was considered. Taking this rotor to be operating at a non-dimensional height of $\frac{Z}{R} = 0.5$, or one-half of a rotor radius above a ground plane, a ground plane is placed parallel to the plane of the rotor at $\frac{Z}{R} = -0.5$. Since the values of induced velocity ratio as given by Castles and De Leeuw are based on a semi-infinite cylindrical vortex sheet, a rotor system assumed to be operating at the ground plane and parallel to the primary rotor, with the same wake angle, is superimposed on the primary system, but with its influence taken to be opposite to that of the primary system. Thus, the combined magnitudes of the induced velocity ratio at the points along the longitudinal axis of the primary rotor is equal to the induced velocities that would result not from a semi-infinite vortex sheet, but from one extending at a wake angle of 45° only to the ground plane, at a vertical height of $\frac{Z}{R} = 0.5$. However, it is necessary that the boundary condition

$$\frac{V_i}{V_{i_{mean}}} = 0 \quad \text{at } \frac{Z}{R} = -0.5$$

be satisfied, that is, that there be no normal component of induced velocity at the ground plane. In order to satisfy this requirement, a mirror image of the two rotor systems, as previously described, is assumed to exist below the ground plane. The influence of the image systems on points along the longitudinal axis of the real rotor is now opposite to that of their counterparts which are above the ground plane. By combining the vortex systems above and below the ground plane, the vortex or wake system as shown in Figure 6 is obtained. It is composed of the actual rotor vortex system, plus three additional vortex systems, with the resultant effect of a rotor operating at the given wake angle of forty-five degrees, and at a height above the ground of half a rotor radius.

By combining the values of the induced velocity ratios, as they exist for each of the four rotor vortex systems at any point along the longitudinal axis of the actual rotor, the net result is now the normal component of induced velocity at that point for the particular rotor in ground effect divided by the mean value of induced velocity out of ground effect, or $\frac{V_{i\ IGE}}{V_{i\ OGE\ mean}}$. The values of induced velocity in ground effect were obtained for points in the longitudinal axis at $\frac{X}{R} = -1.0$, -0.9, -0.8, -0.6, -0.4, -0.2, 0.0, 0.2, 0.4, 0.6, 0.8, 0.9, and 1.0, and have been tabulated in Table 1. Values at these points were determined for rotors operating at the same wake angle, but at heights above the ground plane of $\frac{Z}{R} = 0.6$, 0.8, and 1.0 also, and are found tabulated in Table 1.

In the manner indicated, and for a rotor operating at each of the four heights above the ground as mentioned above, the variation of the normal component of induced velocity along the longitudinal plane of symmetry was determined for rotors operating with wake angles of $\chi = 0.00$, 14.04, 26.56, 45.00, and 63.43 degrees; that is, for wake angles having tangents of 0, $\frac{1}{4}$, $\frac{1}{2}$, 1, and 2, as presented in reference (2). All values of the induced velocity ratio as determined are tabulated in Table 1 and have been plotted in Figures 7(a) to 7(e), together with the distribution given in reference (2) for a rotor with that same wake angle, but not in ground effect.

In considering rotor disks that had a triangular load distribution, the procedure followed was identical to that previously described except that, in this case, reference (3) provided the basic information needed for the induced velocity distribution in the vicinity of a lifting rotor with triangular disk loading. The data obtained were for the same rotor conditions of height above the ground plane and wake angles as determined for the uniformly loaded rotors, except that reference (3) did not contain information pertaining to a wake angle of 14.04 degrees. Consequently, no information of a rotor in ground effect, with a wake angle of 14.04 degrees was obtained for the case of triangular disk loading. The results of the analysis involving rotors with triangular disk loadings, in ground effect, are tabulated in Table 2, and have been plotted in Figures 8(a) to 8(d). The induced velocity distribution for a rotor of corresponding wake angle and out of ground effect, as given by reference (3), is shown in the same figures.

CHAPTER III

RESULTS AND DISCUSSION

The basic results of this investigation, as presented graphically by Figures 7 and 8, show that the effects of ground proximity on the normal component of induced velocity along the longitudinal axis of a lifting rotor are considerable, regardless of the type of disk load distribution assumed. In the case of the uniformly loaded rotor in ground effect, the induced velocities in general become more uniformly distributed along the longitudinal axis of the rotor as the wake angle, and hence forward speed, increases. For the triangular loading, ground effect essentially causes the induced velocities along the rotor to decrease, but the distribution remains similar to the distribution for the rotor out of ground effect.

In order that an indication might be obtained of the accuracy of the reflection method, as it was applied in this study, a comparison of results for uniform disk loading was made with those obtained by Knight and Hefner in reference (5) for the case of a rotor in ground effect with a wake angle equal to zero. The comparison is shown in Figure 9, and is seen to reflect satisfactory agreement for this extreme case.

An alternate analysis of the results of this investigation was made in the form Heyson used in reference (1), additionally, direct comparisons were made with the results by Heyson in which the induced velocities were considered for a point at the rotor center. Since a uniformly loaded rotor was used in reference (1), the results that are given in Figures 7(a) to 7(e) corresponding to that loading were used in the comparison.

It was necessary to re-express the data contained in Figures 7(a) to 7(e) in order to proceed with the comparison. First, a mean value was obtained from each of the graphs of the induced velocity ratio, ${V_{i}}_{IGE}/{V_{i}}_{OGE_{mean}}$, thus giving one value,

$$\frac{{V_{i}}_{IGE_{mean}}}{{V_{i}}_{OGE_{mean}}}$$

for each rotor height at each wake angle. The mean values have been tabulated in Table 3, together with the values of induced velocity ratio as given by Heyson for the center point of the rotor,

$$\frac{{V_{i}}_{IGE_{center}}}{{V_{i}}_{OGE_{center}}}$$

and have been plotted versus wake angle in Figure 10. From this comparison, it is seen that the assumption given by Heyson which stated the average induced velocity over the disk remains proportional to the induced velocity at the center, for a rotor in ground effect, appears to be quite approximate.

In order to present the results of this paper in the manner used in reference (1), it was necessary to work primarily with the data that were obtained for a uniformly loaded rotor disk, the same loading used in reference (1). The first comparison with Heyson's results is one of the ground interference velocity which entails a graph of

$$\frac{\Delta V_{i_{center}}}{V_{i_{OGE_{center}}}} \quad \text{versus} \quad \frac{Z}{R}$$

for each χ , where ΔV_i is the interference velocity or the change in induced velocity caused by ground effect. Using the mean values of induced velocity ratios determined for ground effect, a ratio comparable to Heyson's is

$$\frac{\dfrac{V_{i_{OGE_{mean}}}}{V_{i_{OGE_{mean}}}} - \dfrac{V_{i_{IGE_{mean}}}}{V_{i_{OGE_{mean}}}}}{\dfrac{V_{i_{OGE_{mean}}}}{V_{i_{OGE_{mean}}}}} = \frac{\Delta V_{i_{mean}}}{V_{i_{OGE_{mean}}}}$$

The resulting graph for the present study is shown in Figure 11 adjacent to that given by Heyson. It is seen that the mean interference velocity along the longitudinal axis does not vary with wake angle to the same extent as the interference velocity value at the center of the rotor, and that the average interference velocity along the longitudinal axis of the rotor appears to be less than the value for the center of the rotor.

The second comparison with Heyson's results shows the ground effect on the ratio of nondimensional ground-effect interference velocity in forward flight to the similar velocity in hovering. That is,

$$\frac{\dfrac{V_{i_{center}}}{V_{i_{OGE_{center}}}}}{\left(\dfrac{V_{i_{center}}}{V_{i_{OGE_{center}}}}\right)_{\chi=0}} \quad \text{versus} \quad \frac{Z}{R}$$

Such a ratio for the results of the present paper would be

$$\frac{\dfrac{V_{i_{mean}}}{V_{i_{OGE_{mean}}}}}{\left(\dfrac{V_{i_{mean}}}{V_{i_{OGE_{mean}}}}\right)_{\chi=0}} \quad \text{versus} \quad \frac{Z}{R}$$

The resulting curves are presented along with the equivalent curves from reference (1), in Figure 12. Comparison indicates that the ratio of the mean nondimensional interference velocity divided by the nondimensional interference velocity at conditions of zero wake angle has less of a variation with wake angle, and has less variation with height above the ground, than that shown for the equivalent ratios presented for the midpoint in the rotor.

The next graph which was constructed is a plot of the ground induced interference velocity as a function of forward speed, V. Specifically, Heyson presented plots of

$$\frac{V_{i\ center}}{\left(V_{i\ OGE\ center}\right)_{\chi=0}} \quad \text{versus} \quad \frac{V}{\left(V_{i\ OGE\ center}\right)_{\chi=0}} \quad \text{and } \chi$$

In terms of the results of this paper, these ratios would correspond to

$$\frac{V_{i\ mean}}{\left(V_{i\ OGE\ mean}\right)_{\chi=0}} \quad \text{versus} \quad \frac{V}{\left(V_{i\ OGE\ mean}\right)_{\chi=0}} \quad \text{and } \chi$$

In reference (1), it was shown that the ratio

$$\frac{V_{i\ OGE\ center}}{\left(V_{i\ OGE\ center}\right)_{\chi=0}} = (\text{Cos } \chi)^{\frac{1}{2}}$$

for a rotor operating at zero angle of attack. Then for the present paper, the equivalent expression becomes

$$\frac{V_{i\ OGE\ mean}}{\left(V_{i\ OGE\ mean}\right)_{\chi=0}} = (\text{Cos } \chi)^{\frac{1}{2}}$$

Since the above mentioned ratios as plotted by Heyson were not for constant wake angles, the value of $V_{i\ mean}$ when compared to $\left(V_{i\ mean}\right)_{\chi=0}$ must be corrected by use of the factor $(\text{Cos } \chi)^{\frac{1}{2}}$ in order to allow for wake angle variation. Thus:

$$\frac{V_{i_{mean}} \; (\text{Cos } \chi)^{\frac{1}{2}}}{\left(V_{i_{OGE_{mean}}}\right)_{\chi=0}}$$

is the ratio of the ordinate that must be used. In the determination of the proper abscissa ratio, an expression for V, the forward velocity, is determined from the expression given for χ, where

$$\chi = \text{Tan}^{-1} \frac{- V \text{ Cos } \alpha}{(V \text{ Sin } \alpha - V_i)}$$

Since $\alpha = 0$ in the case considered by Heyson,

$$\chi = \text{Tan}^{-1} (V/-V_{i_{OGE}})$$

or

$$\text{Tan } \chi = (V/-V_{i_{OGE_{mean}}})$$

and

$$\frac{V}{\left(V_{i_{OGE_{mean}}}\right)_{\chi=0}} = - \frac{V_{i_{OGE_{mean}}}}{\left(V_{i_{OGE_{mean}}}\right)_{\chi=0}} \quad (\text{Tan } \chi)$$

Then, as was the case for the ordinate, correction must be made for the variation of $V_{i_{OGE_{mean}}}$ with wake angle χ; therefore,

$$\frac{V(\text{Cos}\ \chi)^{\frac{1}{2}}}{\left(V_{i\ \text{OGE}\ \text{mean}}\right)_{\chi=0}} = - \frac{V_{i\ \text{OGE}\ \text{mean}}}{\left(V_{i\ \text{OGE}\ \text{mean}}\right)_{\chi=0}} (\text{Cos}\ \chi)^{\frac{1}{2}}\ \text{Tan}\ \chi$$

The graph resulting from these ratios is shown with that given by Heyson, and appears in Figure 13. It is apparent that the average ground effect interference velocity along the longitudinal axis of a rotor is not as great as indicated for a point at the center of the rotor, and that the decrease in the average interference velocity is not as rapid with increasing forward speed as would appear from Heyson's analysis for a point at the rotor center.

In the final comparison with the results of Heyson, total induced velocity ratios are plotted versus forward speed for different rotor heights above the ground plane. In this case, reference (1) shows a plot of

$$\frac{V_{i\ \text{IGE}}}{\left(V_{i\ \text{OGE}\ \text{center}}\right)_{\chi=0}} \quad \text{versus} \quad \frac{V}{\left(V_{i\ \text{OGE}\ \text{center}}\right)_{\chi=0}} \quad \text{and}\ \chi$$

for various values of rotor height above the ground plane. In the comparison then,

$$\frac{V_{i\ \text{IGE}\ \text{mean}}\ (\text{Cos}\ \chi)^{\frac{1}{2}}}{\left(V_{i\ \text{OGE}\ \text{mean}}\right)_{\chi=0}} \quad \text{versus} \quad \frac{V\ (\text{Cos}\ \chi)^{\frac{1}{2}}}{\left(V_{i\ \text{OGE}\ \text{mean}}\right)_{\chi=0}} \quad \text{and}\ \chi$$

was used. The $(\text{Cos } \chi)^{\frac{1}{2}}$ was again used as a correction factor for the reason indicated in the previous case. The results of this comparison are found in Figure 14. The indication that the total induced velocity ratios, within the ground heights considered, initially increase with forward speed is verified. The initial increase of the total induced velocity ratios with forward speed and the magnitude of the effect of the ground plane are less, when the mean value along the longitudinal axis is used, than when the values at the rotor center are used as in reference (1). Also, the ground effect is seen to decrease with forward speed more rapidly for the mean value of induced velocity than for the value at the rotor center.

Although no direct comparison can be made between Heyson's results for the center point of a uniformly loaded rotor and the results obtained in this paper for a rotor with a triangular load distribution, the basis of two of the graphs previously mentioned is again used. Plots of ground induced interference velocity ratios and of total induced velocity ratios are shown as functions of forward velocity for various rotor heights above the ground plane. These graphs are presented in Figures 15 and 16 respectively. With the triangular loading assumed, the results indicate that the interference velocities decrease with increasing forward speed, then increase up to a wake angle of forty-five degrees, then decrease. An exception to this is the case of the rotor operating at $Z/R = 1.0$ above the ground plane. For this case, the interference velocity increases to a wake angle of twenty-six degrees, then decreases.

In Figure 16, the induced velocity ratios are shown to increase to a wake angle of about twenty-six degrees, then decrease until a wake angle of forty-five degrees has been reached, and then increase again reaching a maximum in the vicinity of a wake angle of sixty-three degrees as forward velocity increases. As was the case in Figure 15, the rotor operating at one rotor radius from the ground plane is the exception. The plot of the induced velocity ratio for a rotor height of one rotor radius decreases initially from a wake angle of zero degrees to a wake angle of about forty-five degrees where a minimum is reached, after which the curve conforms to the trend of the others.

CHAPTER IV

APPLICATION OF RESULTS

The results of this paper might be useful in determining the induced power required for a helicopter operating in ground effect. A method for making this determination follows:

If the helicopter is assumed to have a uniformly loaded rotor disk, the normal component of induced velocity at the rotor center for a given flight condition out of ground effect, as given by reference (2), is

$$v = \frac{\frac{1}{2} \Omega R C_T}{(1 - \frac{3}{2}\mu^2) \sqrt{\lambda^2 + \mu^2}}$$

which can be solved by using empirical values for

$$\lambda = \frac{(V \operatorname{Sin} \alpha - v)}{\Omega R}$$

or by iteration, since λ is a function of v. The wake angle is then found for $\mu = V \operatorname{Cos} \alpha / \Omega R$ by

$$\chi = \operatorname{Tan}^{-1} \left(\frac{-\mu}{\lambda}\right)$$

Assuming initially that the same wake angle exists in ground effect, and proceeding to the appropriate curve in Figure 10, the mean value for the induced velocity ratio is obtained.

$$\frac{V_{i_{IGE_{mean}}}}{V_{i_{OGE_{mean}}}} \quad \text{or} \quad \frac{V_{i_{IGE_{mean}}}}{v}$$

Then knowing v from above, $V_{i_{IGE_{mean}}}$ is used to determine a corrected value for the wake angle.

$$\chi_{IGE} \approx \mathrm{Tan}^{-1} \frac{\mu \, \Omega \, R}{V \sin \alpha - V_{i_{IGE_{mean}}}}$$

Continuation of this iterative procedure will yield a final value for $V_{i_{IGE_{mean}}}$, which will allow for the determination of induced power required from the relation $P_i = T \, V_{i_{IGE_{mean}}}$.

Should it be preferred that a triangular loading be assumed, an alternate procedure is used. An initial value of χ is found in the same manner as for the case of uniform loading.

Assuming this wake angle to be the same in ground effect, the appropriate curve in Figure 8(a) to 8(d) is selected from which, at the plus and minus X/R = 3/4 points, an average

$$\frac{\left(V_{i_{IGE}}\right)_{3/4\,R}}{V_{i_{ref}}}$$

is determined. Taking $V_{i_{ref}} = v$, $\left(V_{i_{IGE}}\right)_{3/4\,R}$ is calculated and used to determine a new wake angle, where

$$\chi \approx \mathrm{Tan}^{-1} \frac{\mu \, \Omega \, R}{V \, \mathrm{Sin} \, \alpha - \left(V_{i \; IGE} \right)_{3/4 \, R}}$$

This procedure is continued, giving a final value for $\left(V_{i \; IGE} \right)_{3/4 \, R}$ which in turn will allow for the determination of the induced power required in ground effect.

CHAPTER V

CONCLUSIONS

1. The results of this study indicate that the normal component of induced velocity at the center point of a lifting rotor does not appear to be representative of the mean value over the rotor, as was assumed in NASA TN D-234, and that such an assumption would tend to induce error into any estimate of the effect of the ground plane.

2. This analysis indicates that, for rotors in forward flight, the ground effect decreases with height above the ground more rapidly than it does in hovering, but to a lesser extent than indicated by Heyson in NASA TN D-234.

3. Most of the decrease of ground effect on a lifting rotor, with increase in forward speed, is seen to occur at the lower forward speeds. TN D-234 showed this phenomenon to take place to an even greater extent.

4. The present study indicates that, in forward flight, the reduction of ground effect with forward speed is so rapid that, at the heights considered, the mean induced velocity over the rotor increases slightly rather than decreases as the helicopter speeds are increased. This increase is to a lesser degree, however, than is indicated in TN D-234 for the induced velocity at the center of the rotor.

5. The induced velocity distributions along the longitudinal diameter of rotors in ground effect and having a triangular loading were

found to remain similar to the distributions for rotors out of ground effect except that a reduction in magnitude occurred with each reduction of rotor height above the ground.

APPENDIX

Table 1(a). Induced Velocity Distributions for Uniform Disk Loading, $\frac{V_{i_{IGE}}}{V_{i_{OGE_{mean}}}}$

χ	X/R → H/R ↓	-1.0	-0.9	-0.8	-0.6	-0.4	-0.2	0.0	0.2	0.4	0.6	0.8	0.9	1.0
0.0°	0.5	0.573	0.492	0.438	0.292	0.232	0.206	0.195	0.206	0.232	0.292	0.438	0.492	0.573
	0.6	0.615	0.530	0.472	0.379	0.299	0.278	0.258	0.278	0.299	0.379	0.472	0.530	0.615
	0.8	0.676	0.619	0.564	0.485	0.426	0.410	0.408	0.410	0.426	0.485	0.564	0.619	0.676
	1.0	0.699	0.675	0.628	0.555	0.504	0.474	0.466	0.474	0.504	0.555	0.628	0.675	0.699
14.04°	0.5	0.503	0.422	0.350	0.238	0.213	0.205	0.208	0.215	0.247	0.340	0.431	0.535	0.622
	0.6	0.537	0.466	0.412	0.293	0.291	0.275	0.294	0.328	0.376	0.442	0.492	0.586	0.676
	0.8	0.555	0.535	0.522	0.432	0.418	0.415	0.430	0.441	0.480	0.531	0.574	0.659	0.719
	1.0	0.559	0.553	0.549	0.563	0.526	0.495	0.505	0.528	0.543	0.606	0.655	0.732	0.778
26.56°	0.5	0.467	0.437	0.403	0.342	0.300	0.262	0.228	0.204	0.228	0.320	0.428	0.501	0.656
	0.6	0.442	0.474	0.447	0.426	0.343	0.314	0.286	0.291	0.303	0.390	0.502	0.589	0.712
	0.8	0.414	0.447	0.467	0.487	0.471	0.460	0.439	0.439	0.467	0.533	0.635	0.699	0.801
	1.0	0.427	0.463	0.497	0.547	0.545	0.531	0.530	0.533	0.535	0.606	0.701	0.792	0.878

Table 1(b). Induced Velocity Distributions for Uniform Disk Loading, $\frac{V_{i\ IGE}}{V_{i\ OGE\ mean}}$

χ	X/R H/R	-1.0	-0.9	-0.8	-0.6	-0.4	-0.2	0.0	0.2	0.4	0.6	0.8	0.9	1.0
45.00°	0.5	0.133	0.366	0.406	0.361	0.292	0.290	0.305	0.326	0.293	0.319	0.460	0.620	0.847
	0.6	0.142	0.391	0.418	0.404	0.361	0.384	0.390	0.440	0.426	0.452	0.591	0.782	0.950
	0.8	0.146	0.402	0.458	0.469	0.477	0.498	0.490	0.511	0.573	0.645	0.793	0.938	1.159
	1.0	0.155	0.412	0.476	0.507	0.539	0.583	0.591	0.625	0.691	0.788	0.930	1.052	1.285
63.43°	0.5	-0.417	0.220	0.326	0.506	0.652	0.599	0.408	0.216	0.103	0.058	0.505	0.839	1.341
	0.6	-0.429	0.213	0.320	0.512	0.671	0.650	0.557	0.380	0.233	0.168	0.215	0.607	1.234
	0.8	-0.439	0.202	0.306	0.510	0.666	0.703	0.699	0.632	0.477	0.422	0.486	0.721	1.109
	1.0	-0.445	0.197	0.307	0.486	0.624	0.695	0.744	0.792	0.674	0.580	0.635	0.860	1.284

Table 2(a). Induced Velocity Distributions for Triangular Disk Loading, $\frac{V_{i\ IGE}}{V_{i\ ref}}$

χ	X/R H/R	-1.0	-0.9	-0.8	-0.6	-0.4	-0.2	0.0	0.2	0.4	0.6	0.8	0.9	1.0
0.0°	0.5	1.068	0.820	0.595	0.247	-0.080	-0.313	-0.588	-0.313	-0.080	0.247	0.595	0.820	1.068
	0.6	1.134	0.872	0.623	0.287	0.004	-0.292	-0.568	-0.292	0.004	0.287	0.623	0.872	1.134
	0.8	1.233	0.904	0.709	0.375	0.051	-0.253	-0.498	-0.253	0.051	0.375	0.709	0.904	1.233
	1.0	1.288	1.090	0.833	0.510	0.162	-0.170	-0.406	-0.170	0.162	0.510	0.833	1.090	1.288
26.56°	0.5	0.794	0.793	0.654	0.384	0.220	-0.202	-0.540	-0.373	-0.036	0.256	0.647	0.922	1.221
	0.6	0.820	0.824	0.716	0.479	0.236	-0.192	-0.522	-0.340	-0.028	0.265	0.673	1.020	1.295
	0.8	0.815	0.861	0.767	0.559	0.266	-0.184	-0.513	-0.325	0.003	0.278	0.744	1.050	1.445
	1.0	0.831	0.885	0.797	0.596	0.275	-0.179	-0.504	-0.317	0.017	0.286	0.751	1.081	1.430

Table 2(b). Induced Velocity Distributions for Triangular Disk Loading, $\frac{V_{i\ IGE}}{V_{i\ ref}}$

χ	X/R H/R	-1.0	-0.9	-0.8	-0.6	-0.4	-0.2	0.0	0.2	0.4	0.6	0.8	0.9	1.0
45.00°	0.5	0.382	0.518	0.474	0.378	0.156	-0.199	-0.680	-0.484	-0.336	0.010	0.448	0.844	1.349
	0.6	0.390	0.524	0.482	0.422	0.210	-0.122	-0.600	-0.403	-0.291	0.031	0.523	0.920	1.425
	0.8	0.415	0.548	0.535	0.487	0.318	-0.046	-0.519	-0.354	-0.084	0.129	0.574	0.969	1.532
	1.0	0.428	0.566	0.562	0.550	0.365	0.220	-0.465	-0.331	-0.043	0.305	0.798	1.190	1.678
63.43°	0.5	-0.346	0.396	0.621	0.765	0.661	0.235	-0.426	-0.571	-0.502	-0.194	0.269	0.816	1.604
	0.6	-0.358	0.385	0.611	0.778	0.692	0.310	-0.299	-0.458	-0.363	-0.092	0.318	0.824	1.742
	0.8	-0.360	0.385	0.611	0.782	0.713	0.382	-0.175	-0.281	-0.156	0.123	0.562	1.099	1.961
	1.0	-0.369	0.380	0.611	0.792	0.732	0.417	-0.135	-0.212	-0.044	0.320	0.739	1.269	2.146

Table 3. Mean and Center Point Values of Induced Velocity Ratio for Rotors in Ground Effect

H/R	χ=0.0°	14.04°	26.56°	45.00°	63.48°
Mean - Uniform Disk Loading, $\frac{V_{i\ IGE\ mean}}{V_{i\ OGE\ mean}}$					
0.5	0.3096	0.3000	0.3312	0.3616	0.3920
0.6	0.3760	0.3800	0.3936	0.4520	0.4240
0.8	0.4912	0.4896	0.5088	0.5616	0.5456
1.0	0.5568	0.5660	0.5784	0.6560	0.6168
Mean - Triangular Disk Loading, $\frac{V_{i\ IGE\ mean}}{V_{i\ OGE\ mean}}$					
0.5	0.1412	---	0.2080	0.0608	0.1608
0.6	0.1888	---	0.2472	0.1192	0.2232
0.8	0.2496	---	0.2776	0.2032	0.3464
1.0	0.3604	---	0.2952	0.2880	0.4200
Center Point - Uniform Disk Loading, $\frac{V_{i\ IGE\ center}}{V_{i\ OGE\ center}}$					
0.5	0.190	0.200	0.215	0.290	0.516
0.6	0.265	0.275	0.300	0.400	0.645
0.8	0.405	0.420	0.460	0.590	0.790
1.0	0.518	0.535	0.580	0.710	0.857

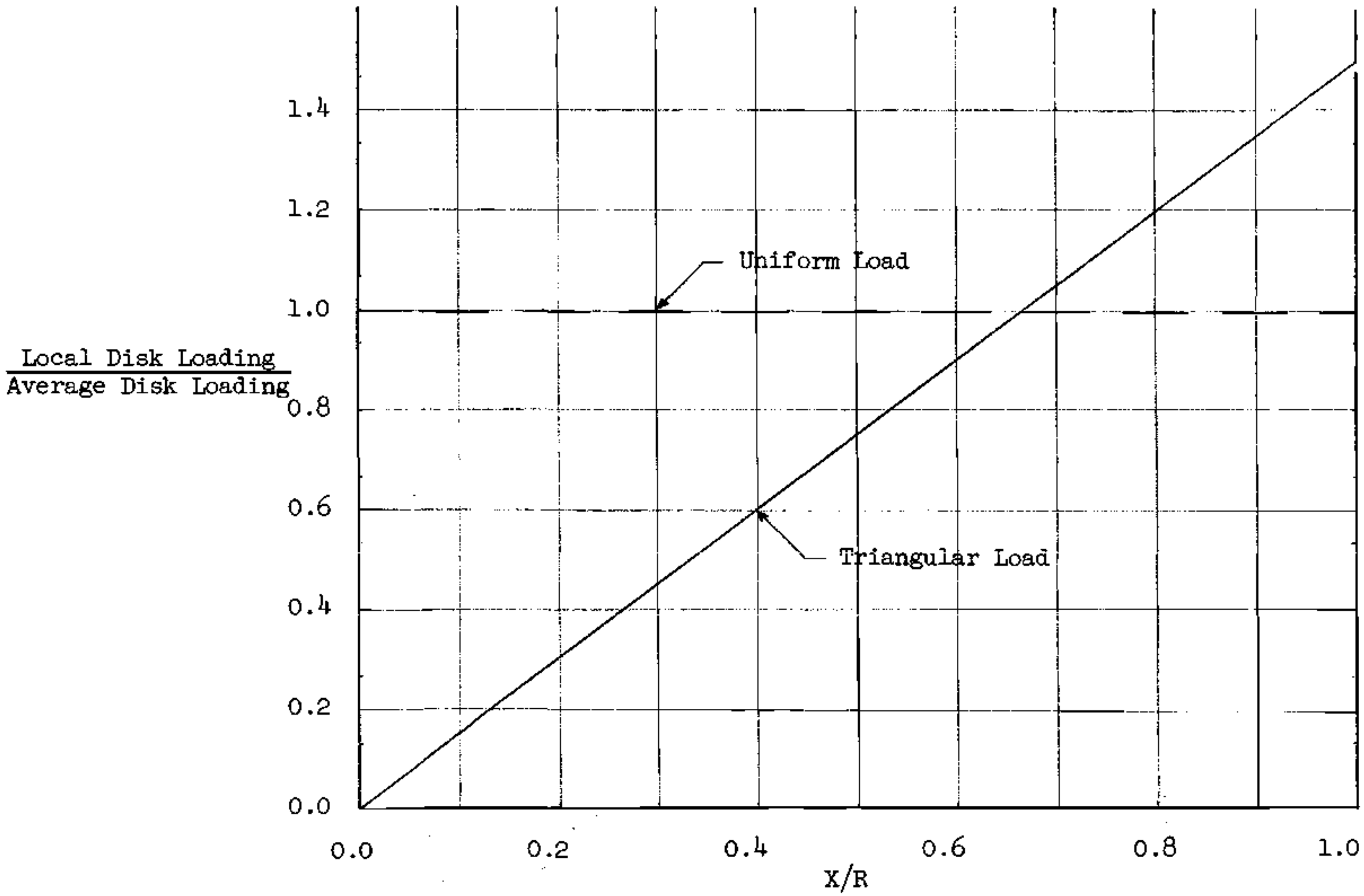

Figure 1. Disk Loadings Considered in Calculations

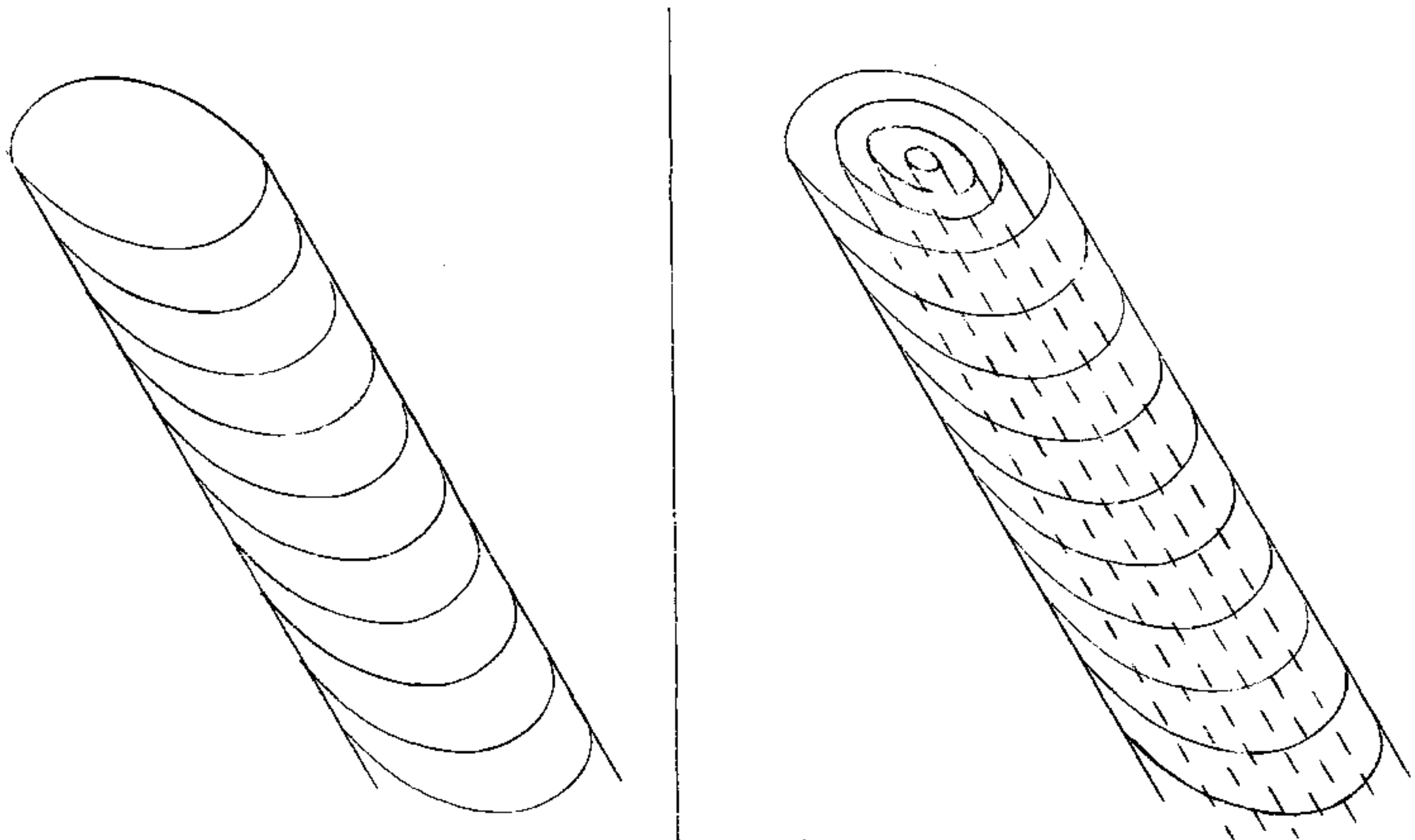

Uniform Load

Non-uniform Axially Symmetric Load

Figure 2. Assumed Vortex Pattern Behind Rotor Out of Ground Effect

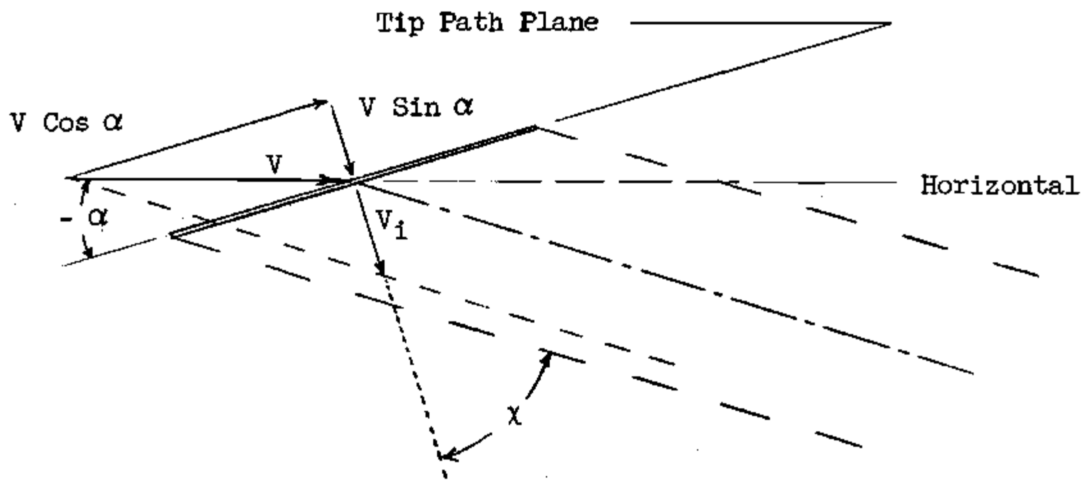

$$\chi = \mathrm{Tan}^{-1} \frac{V \cos \alpha}{V \sin \alpha - V_i} = \mathrm{Tan}^{-1} \left(\frac{-\mu}{\lambda}\right)$$

Figure 3. Geometry of Wake Angle

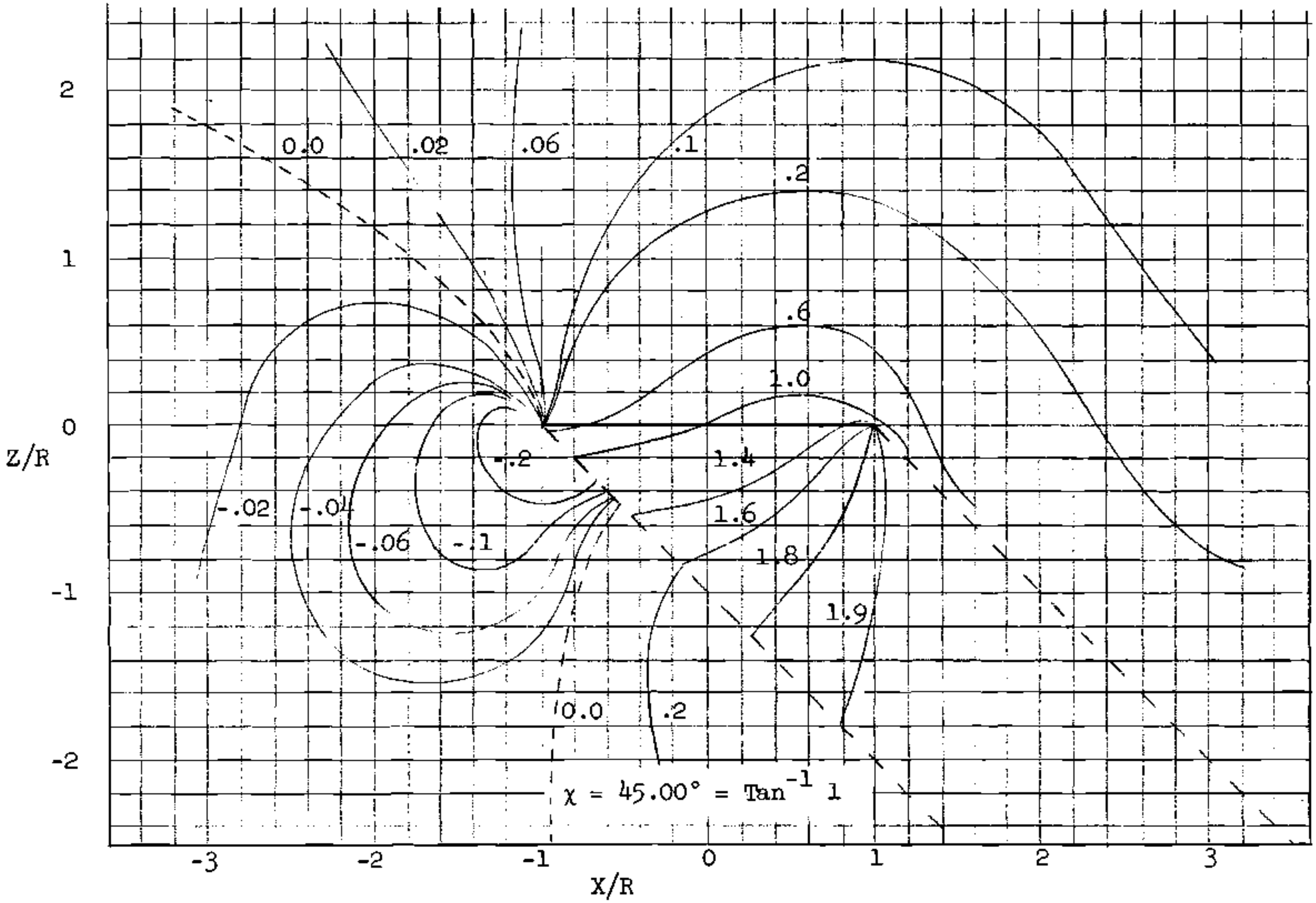

Figure 4. Lines of Constant Induced Velocity Ratio V_i/v in the Longitudinal Plane of Symmetry of a Rotor with Uniform Disk Loading (Reproduced from Ref. 2)

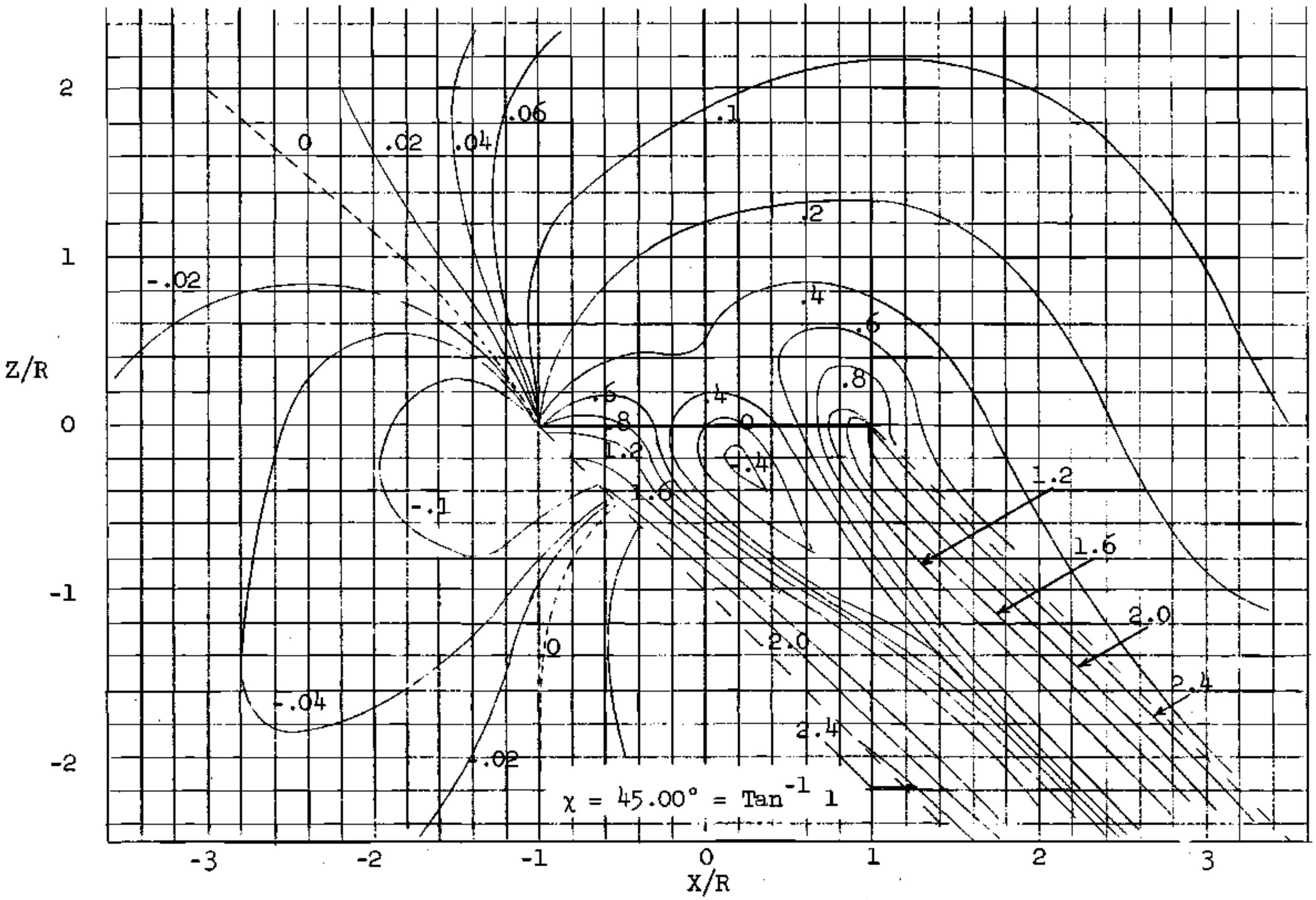

Figure 5. Lines of Constant Induced Velocity Ratio $V_i/V_{i_{ref}}$ in the Longitudinal Plane of Symmetry of a Rotor with a Triangular Disk Loading (Reproduced from Ref. 3)

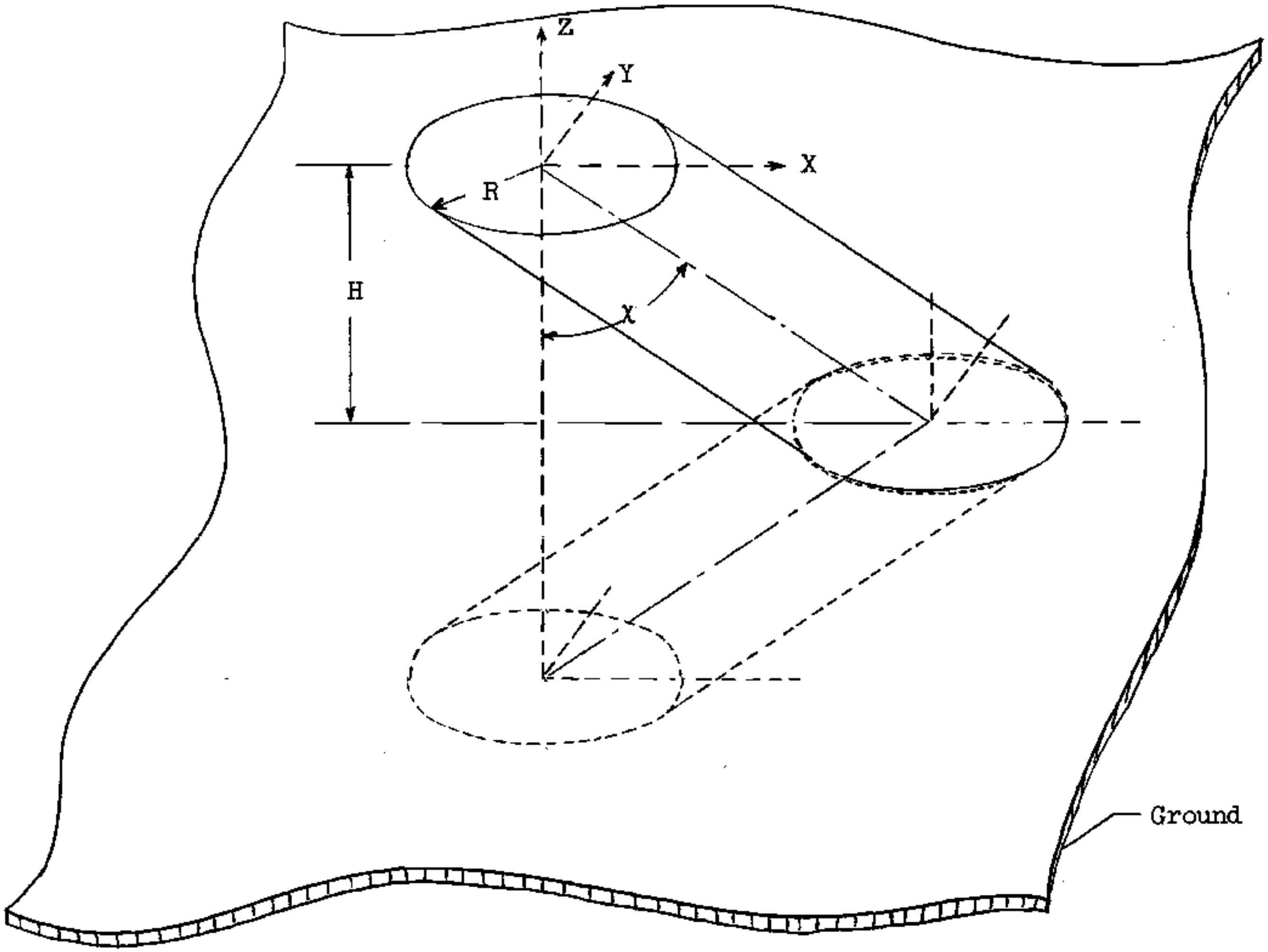

Figure 6. Representation of the Vortex Pattern of a Rotor in Ground Effect

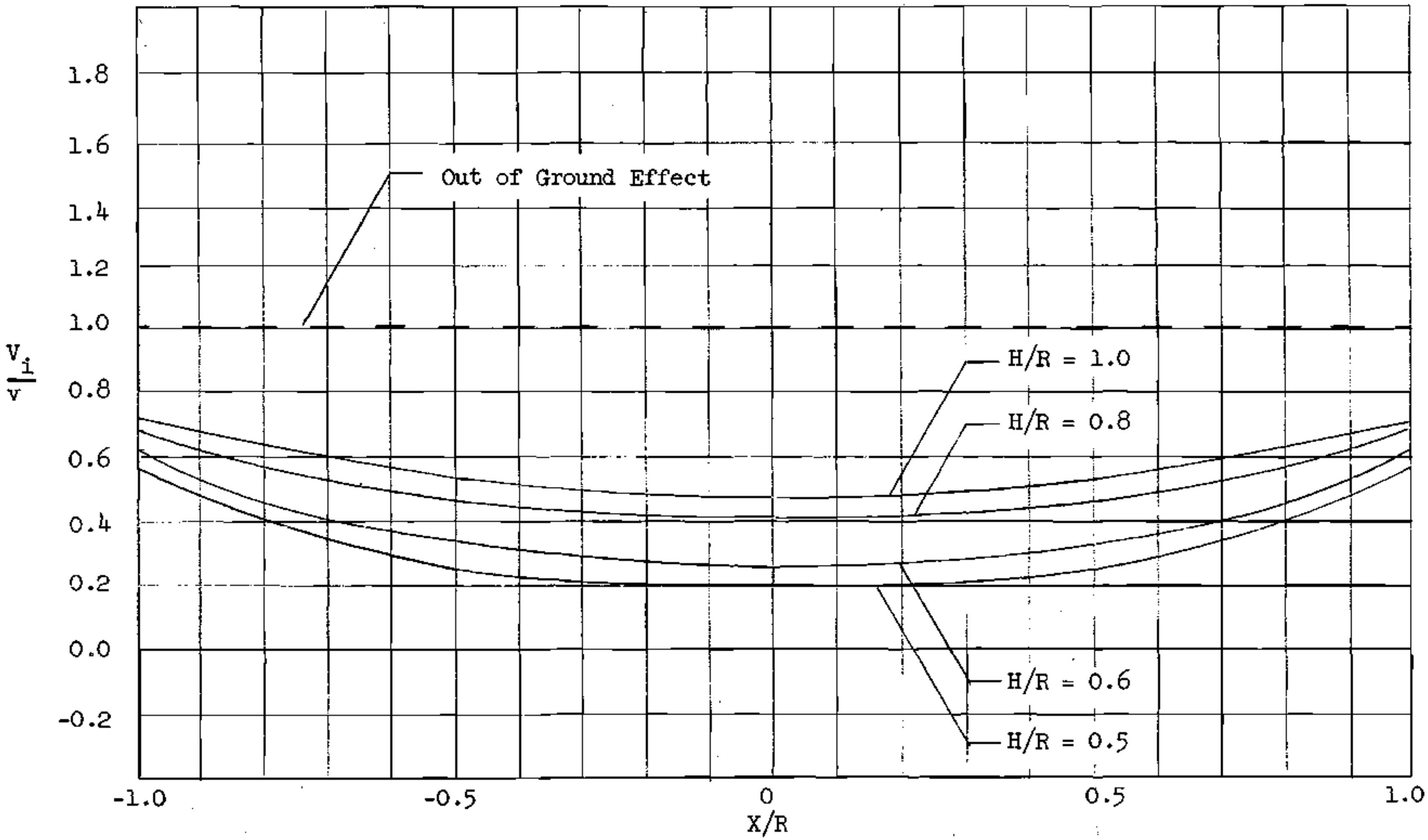

(a) For $\chi = 0.00° = \mathrm{Tan}^{-1}\ 0$

Figure 7. Induced Velocity Distribution Along the Longitudinal Diameter of a Lifting Rotor with a Uniform Disk Loading

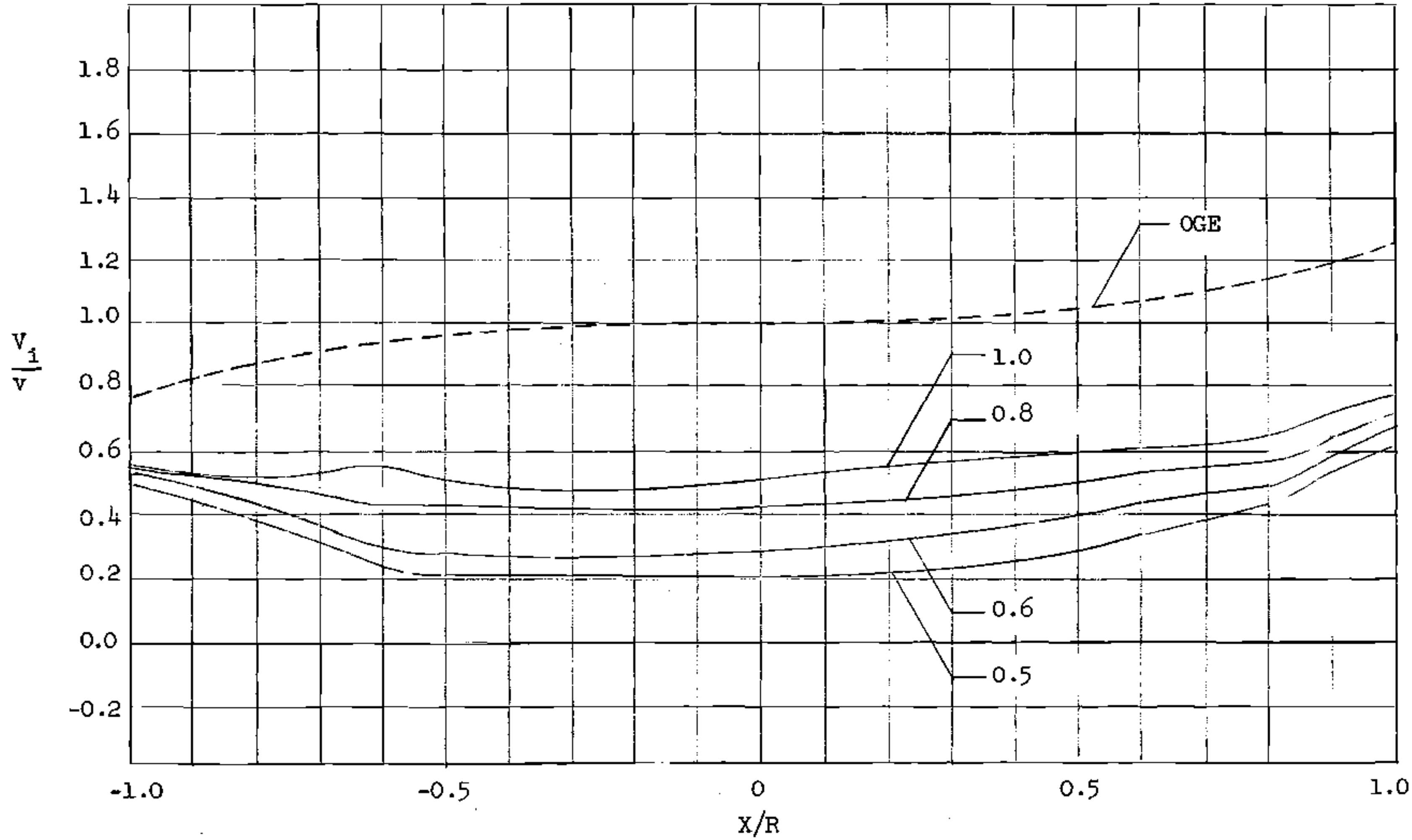

(b) For $\chi = 14.04° = \mathrm{Tan}^{-1}\ 1/4$

Figure 7 (Continued)

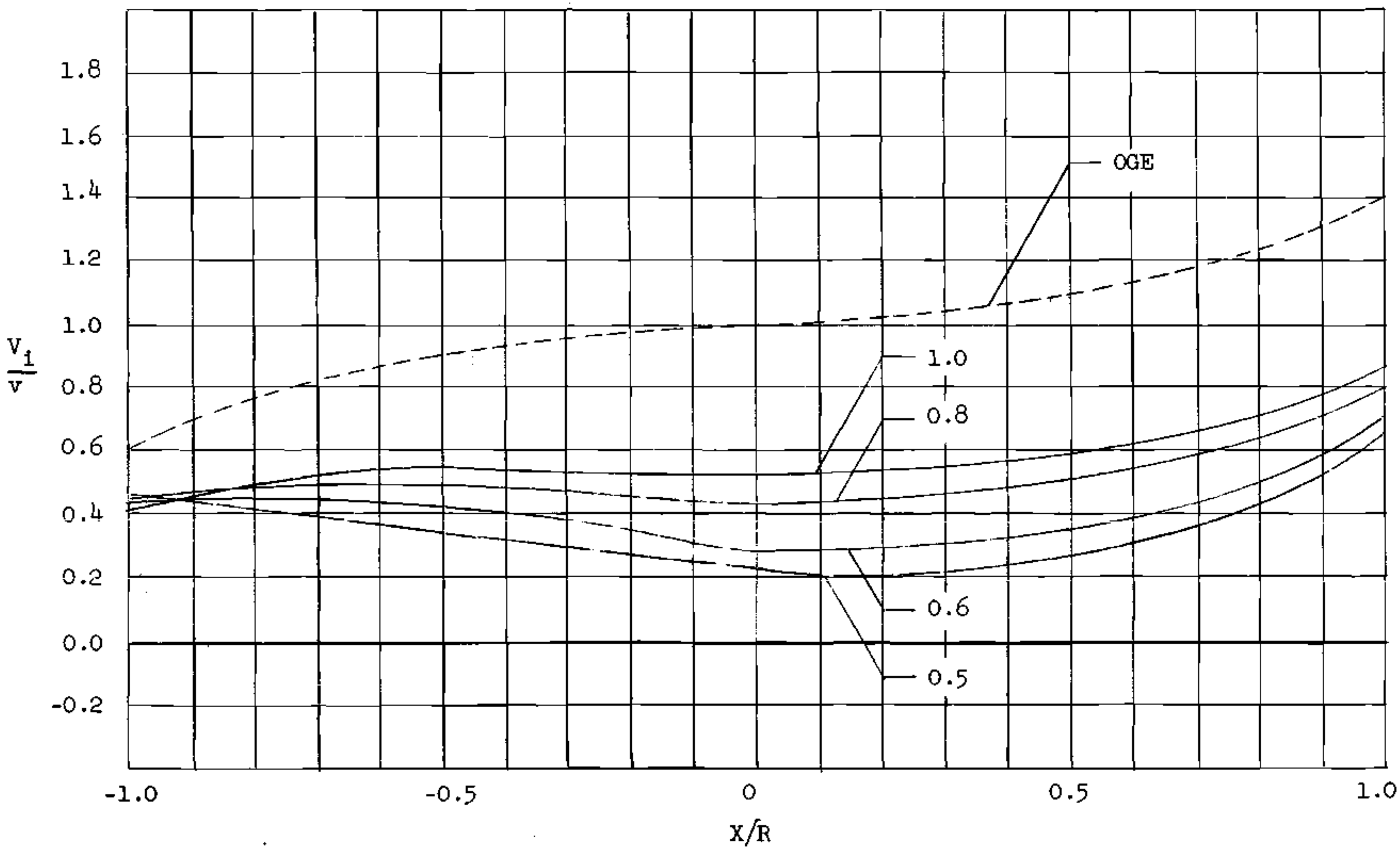

(c) For $\chi = 26.56° = \text{Tan}^{-1}\ 1/2$

Figure 7 (Continued)

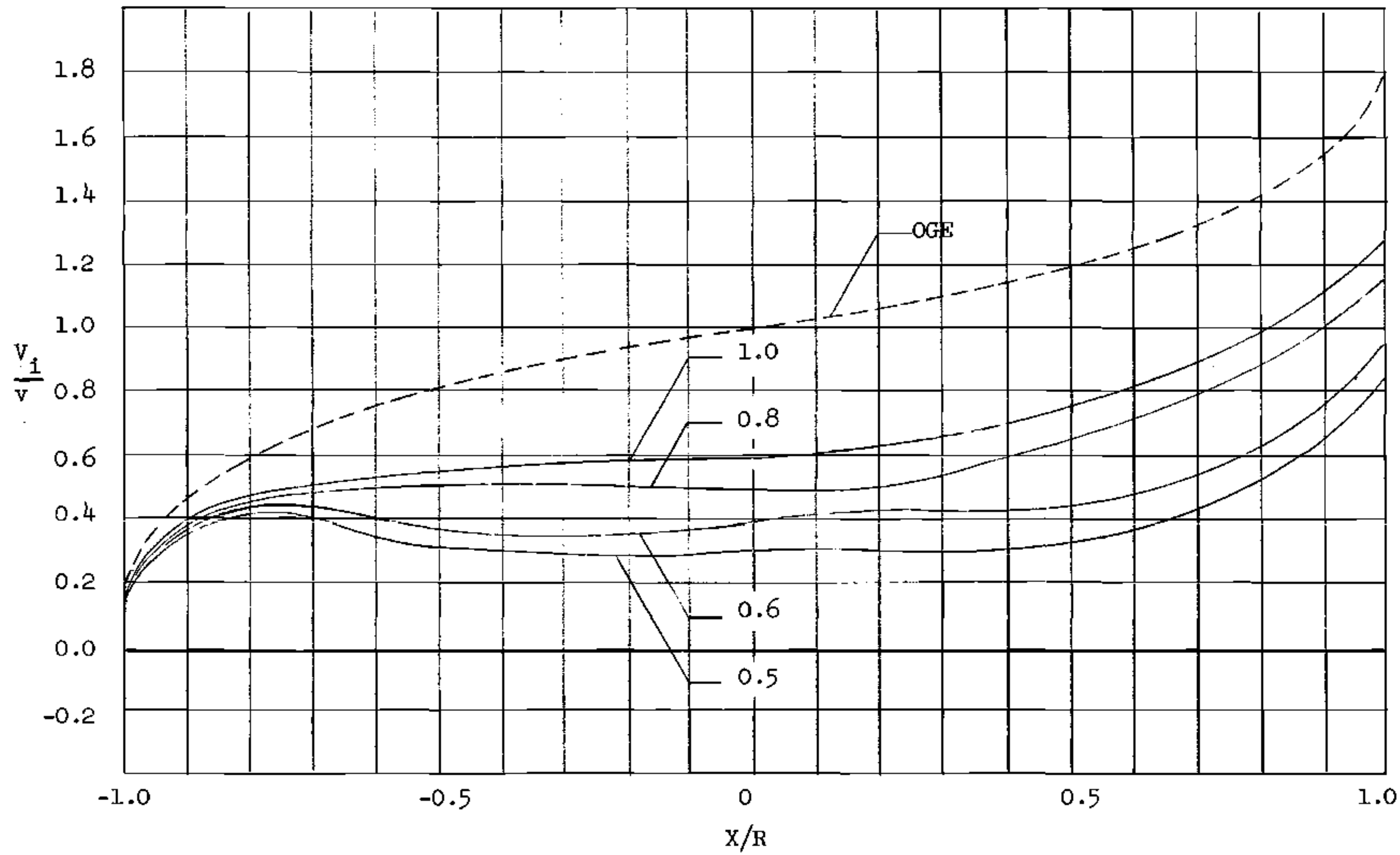

(d) For $\chi = 45.00° = \text{Tan}^{-1}\ 1$

Figure 7 (Continued)

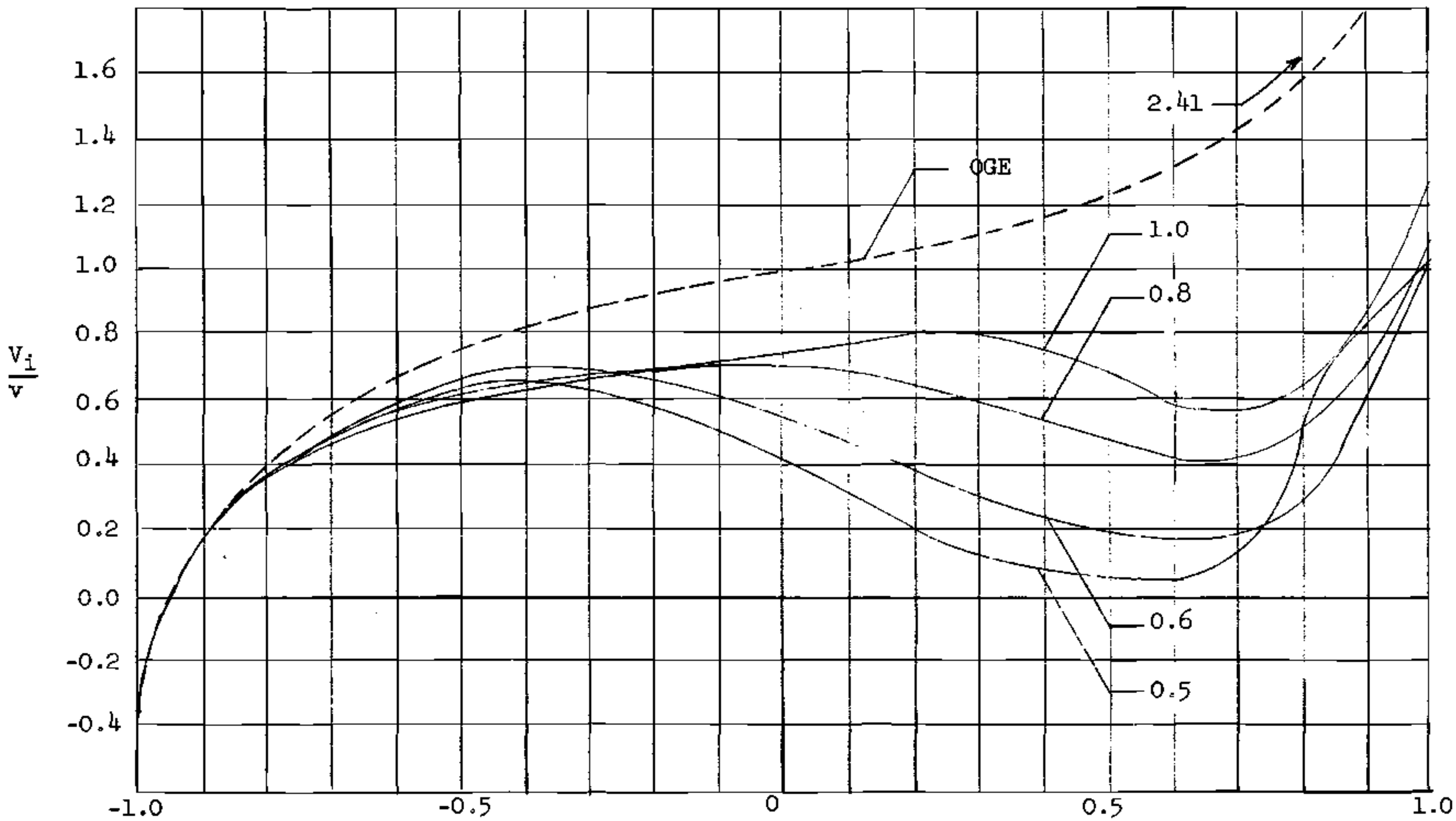

(e) For $\chi = 63.43° = \mathrm{Tan}^{-1} 2$

Figure 7 (Continued)

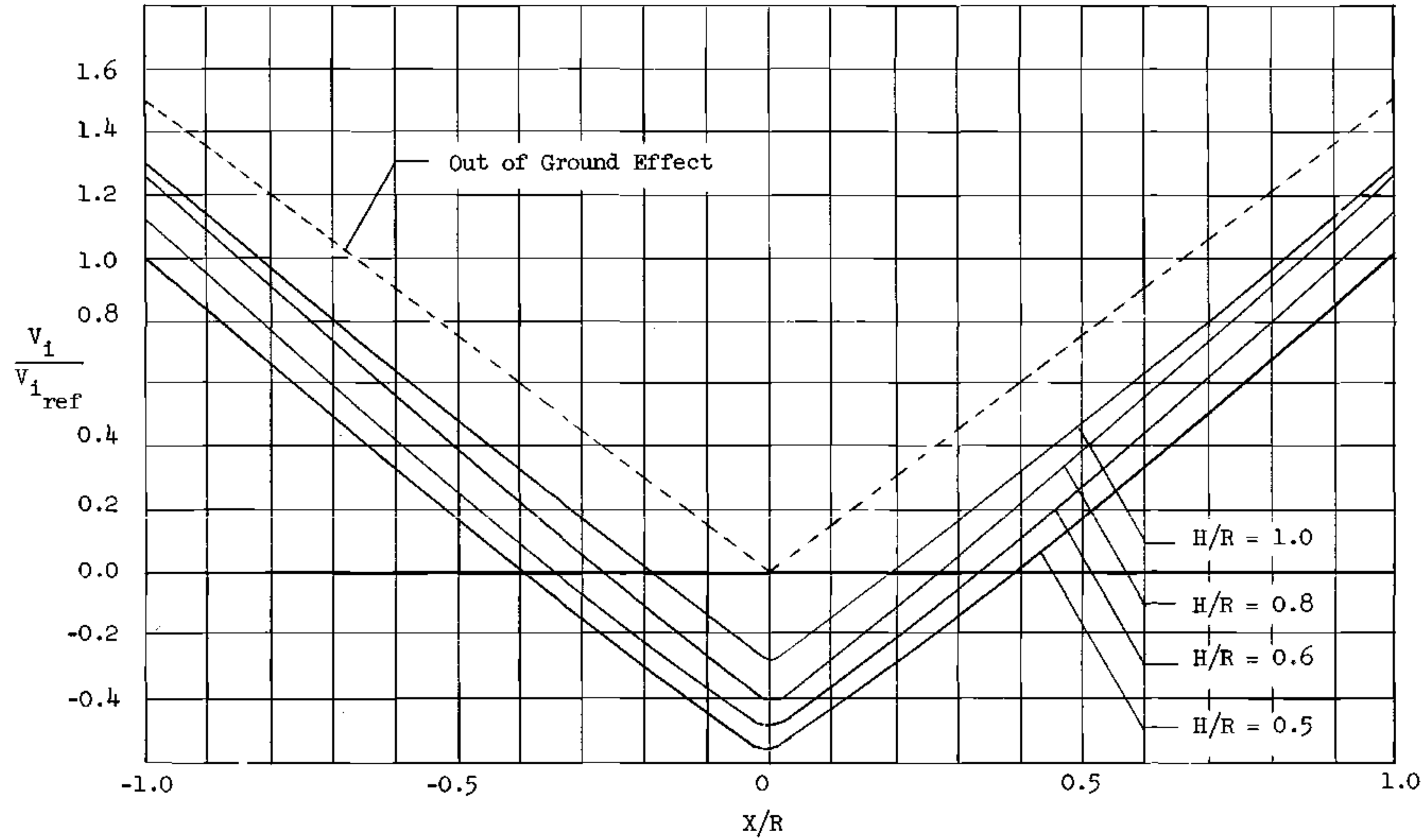

(a) For $\chi = 0.00° = \tan^{-1} 0$

Figure 8. Induced Velocity Distribution Along the Longitudinal Diameter of a Lifting Rotor with a Triangular Disk Loading

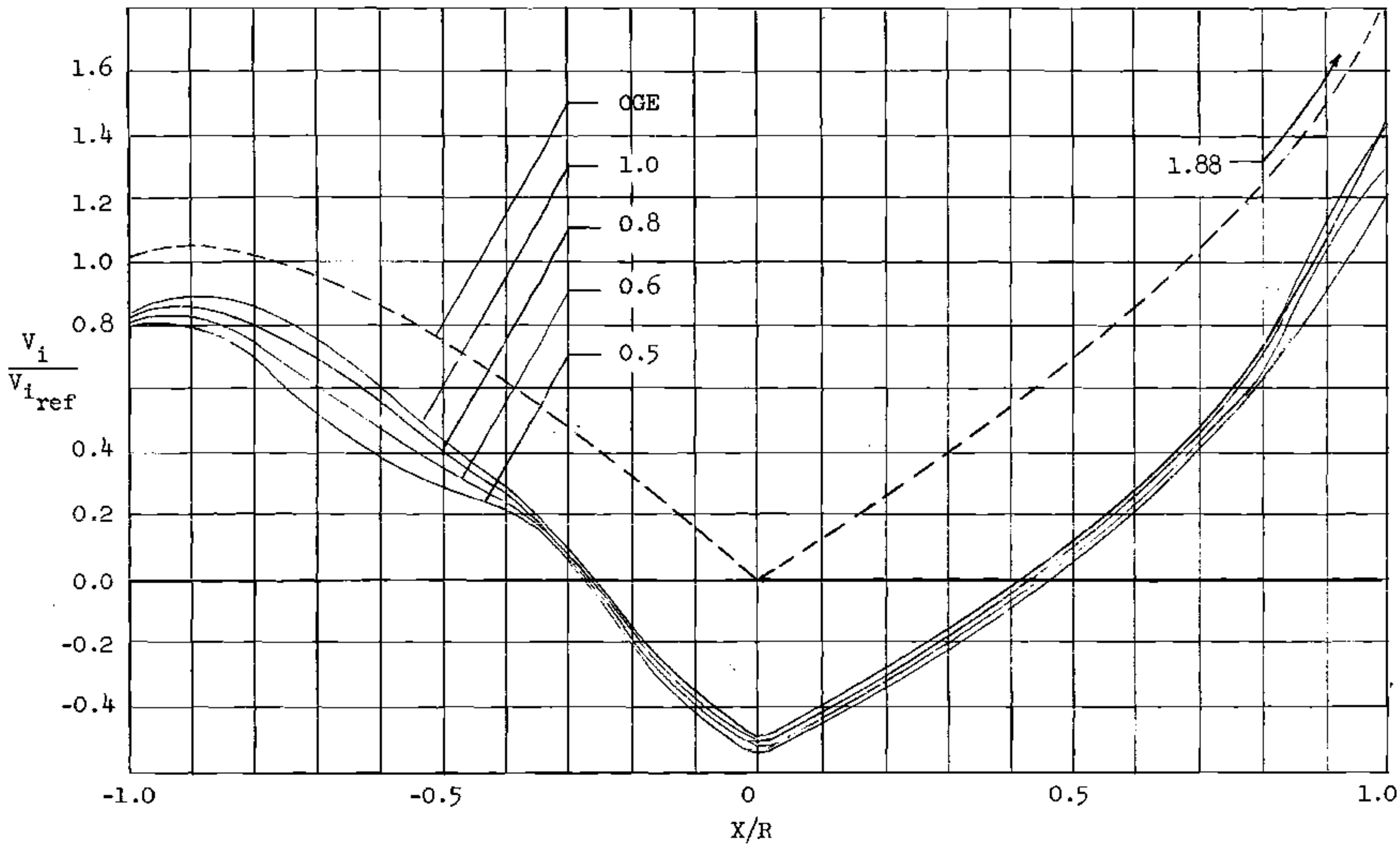

(b) For $\chi = 26.56° = \mathrm{Tan}^{-1}\ 1/2$

Figure 8 (Continued)

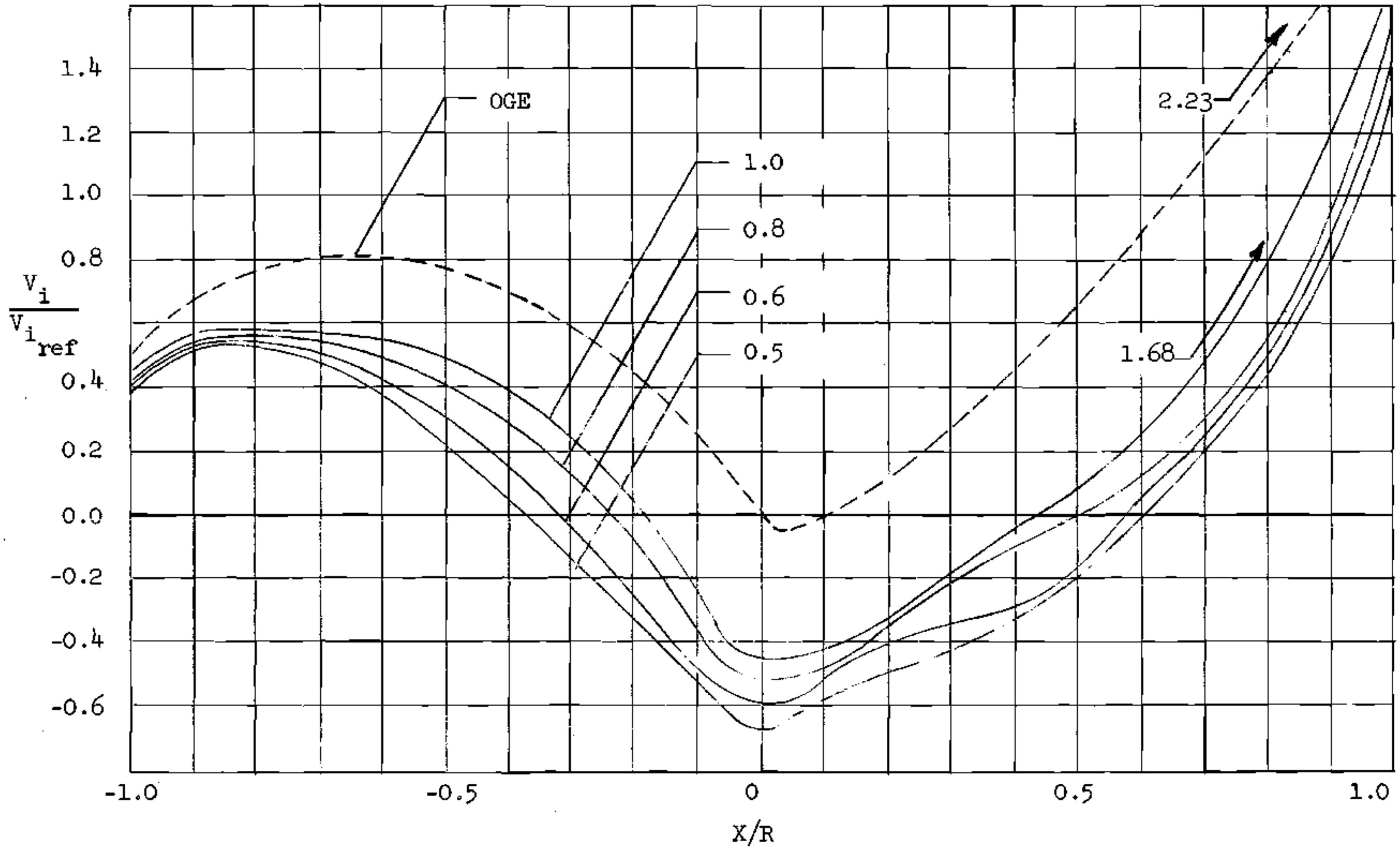

(c) For $\chi = 45.00° = \mathrm{Tan}^{-1}\, 1$

Figure 8 (Continued)

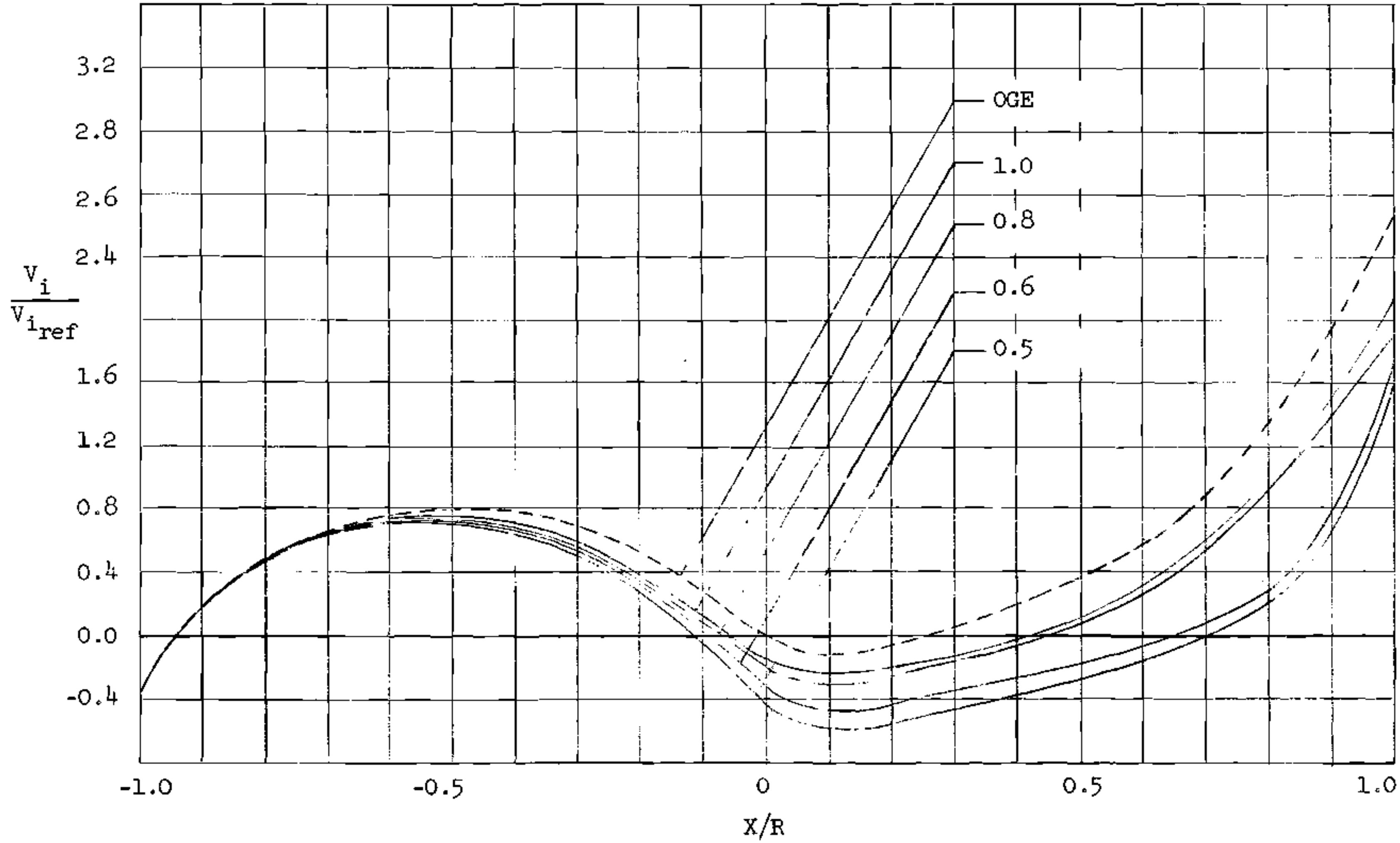

(d) For $\chi = 63.43° = \mathrm{Tan}^{-1}\ 2$

Figure 8 (Continued)

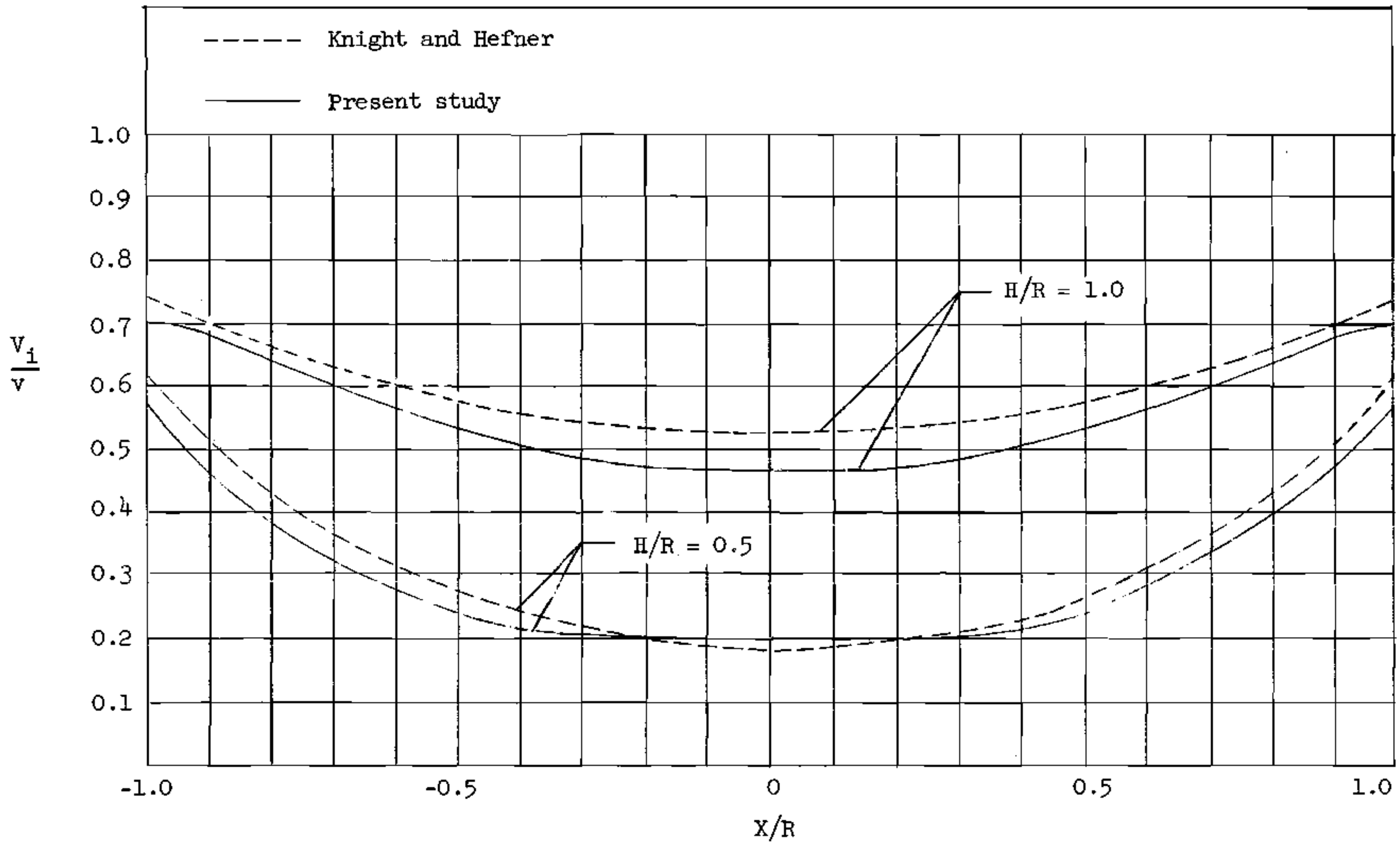

Figure 9. Comparison of Induced Velocity Distributions for Zero Wake Angle--Present Study versus Knight and Hefner (Reference 4)

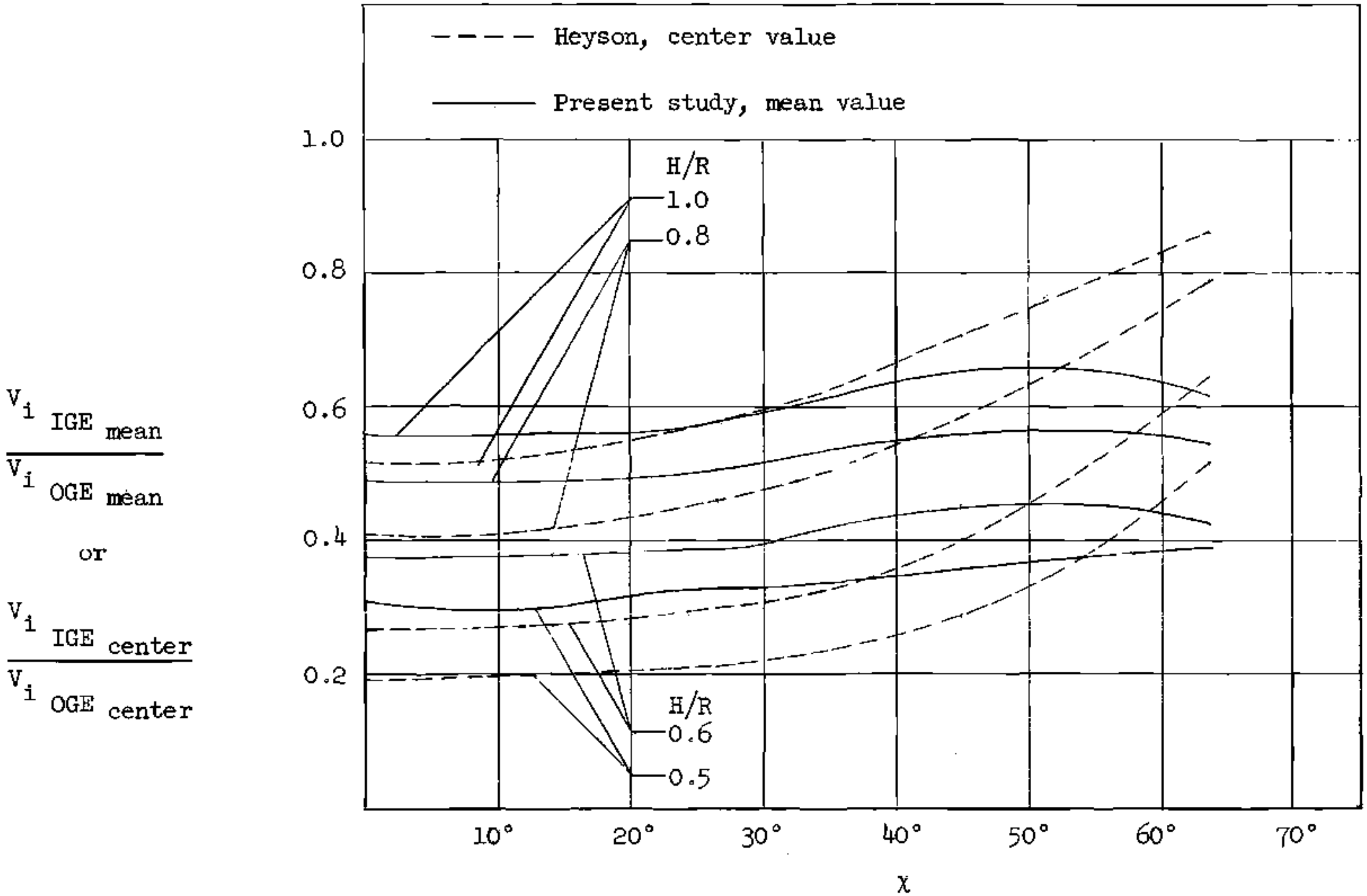

Figure 10. Variation of Mean and Center Values of Induced Velocity Ratios with Wake Angle--Present Study versus Heyson (Reference 1)

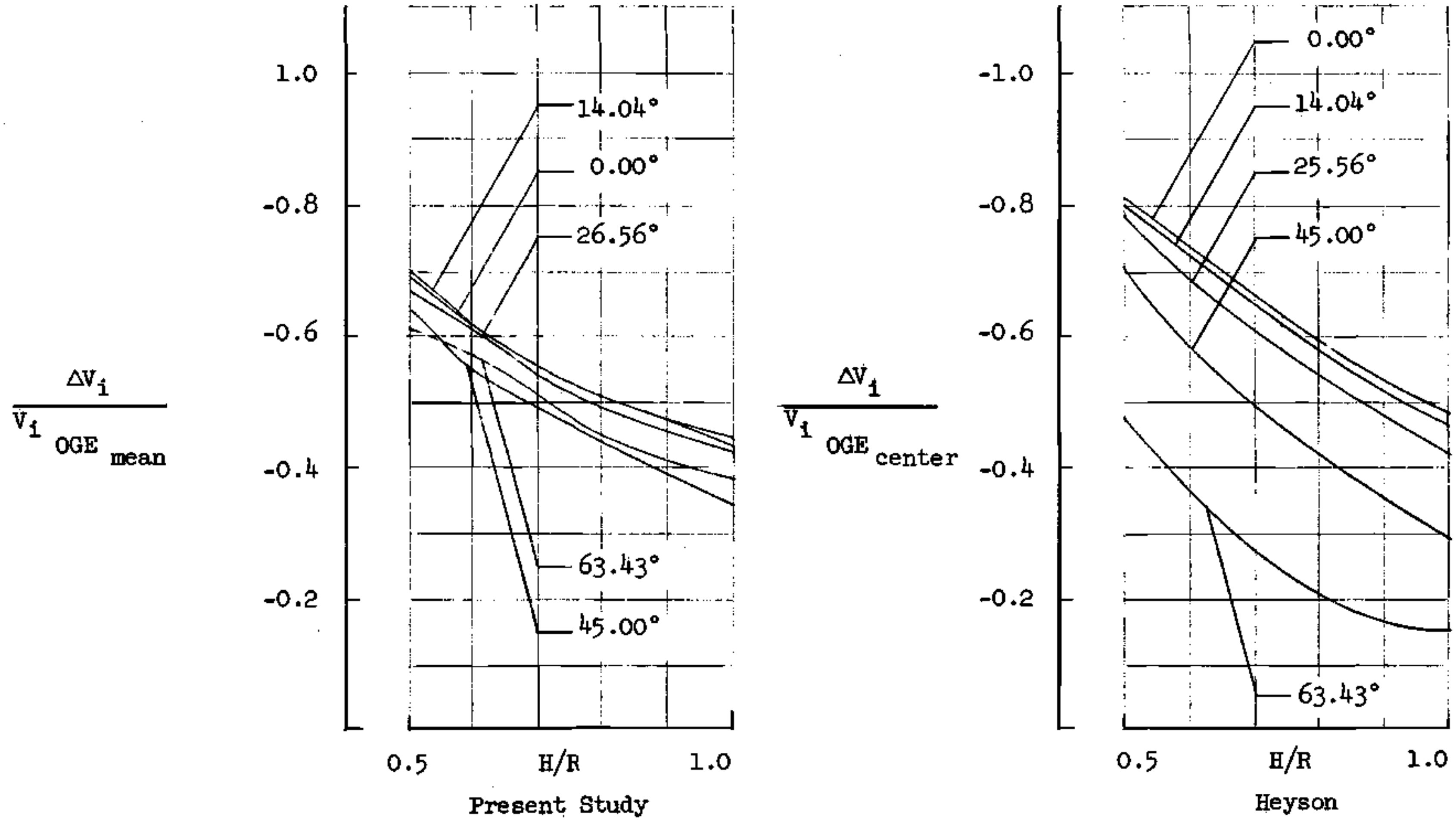

Figure 11. Ground-induced Interference Velocity versus Height Above the Ground

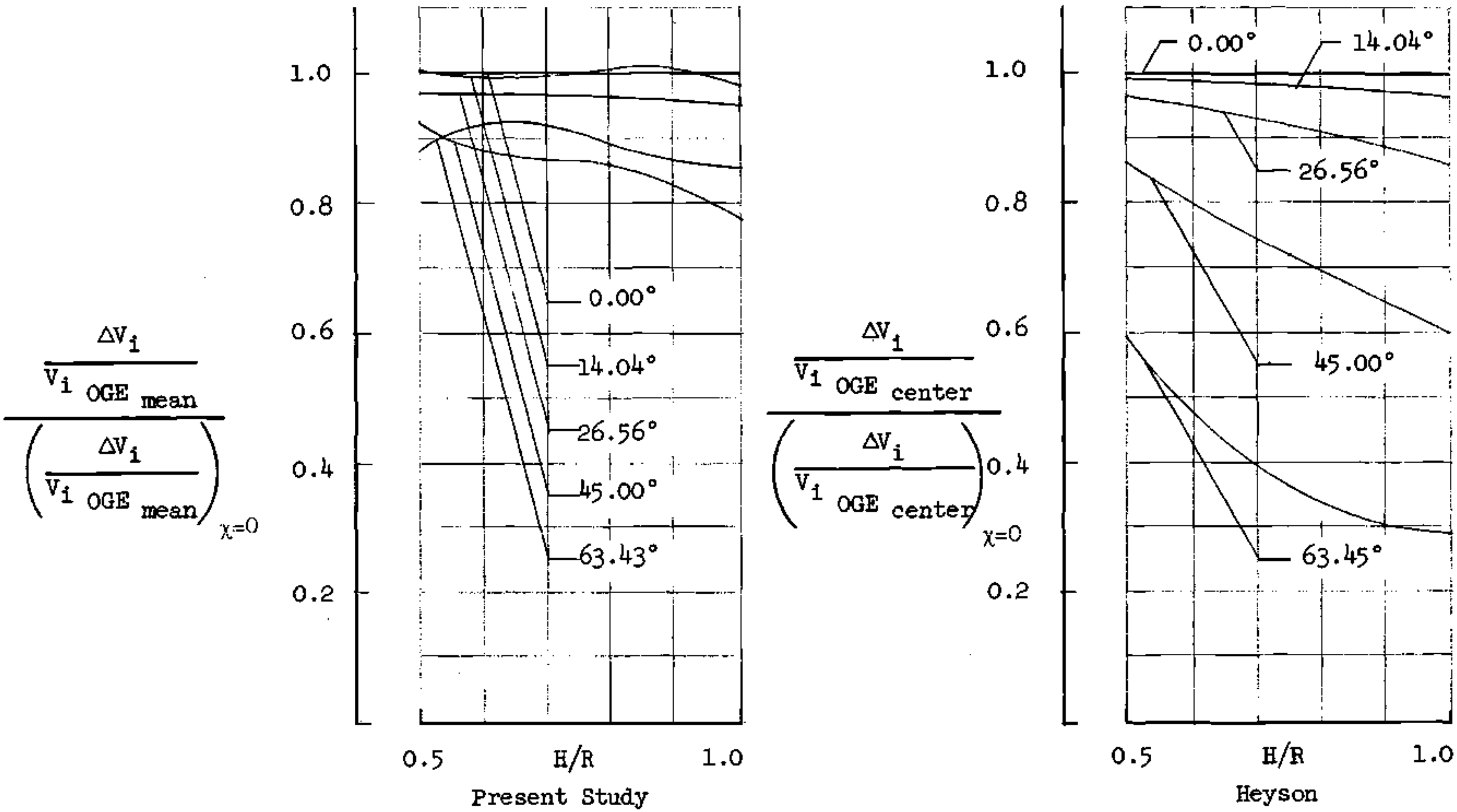

Figure 12. Effect of Ground on Ratio of Nondimensional Ground-Effect Interference Velocity in Forward Flight to the Similar Velocity in Hovering

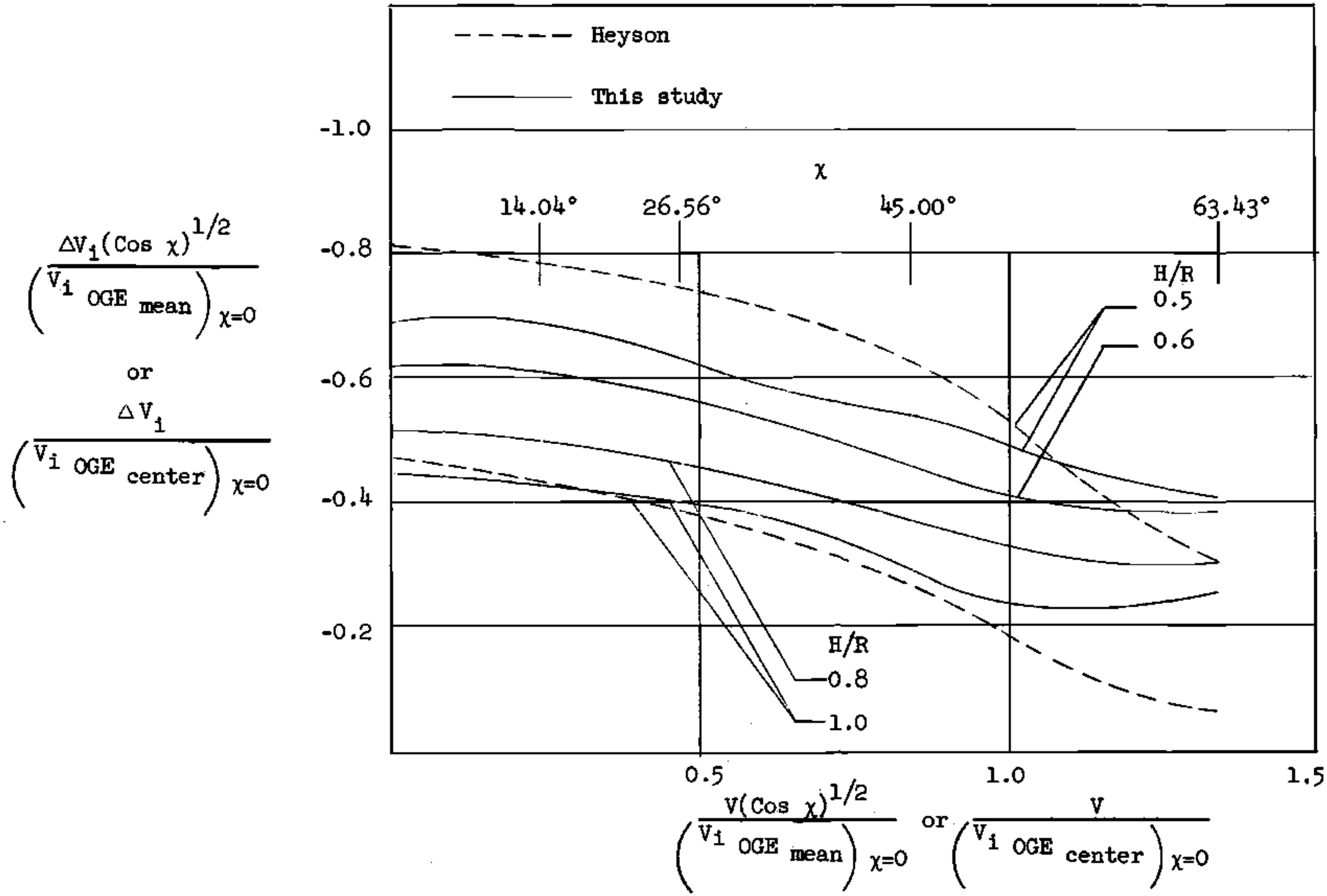

Figure 13. Ground-induced Interference Velocity Versus Forward Speed--Uniform Disk Loading

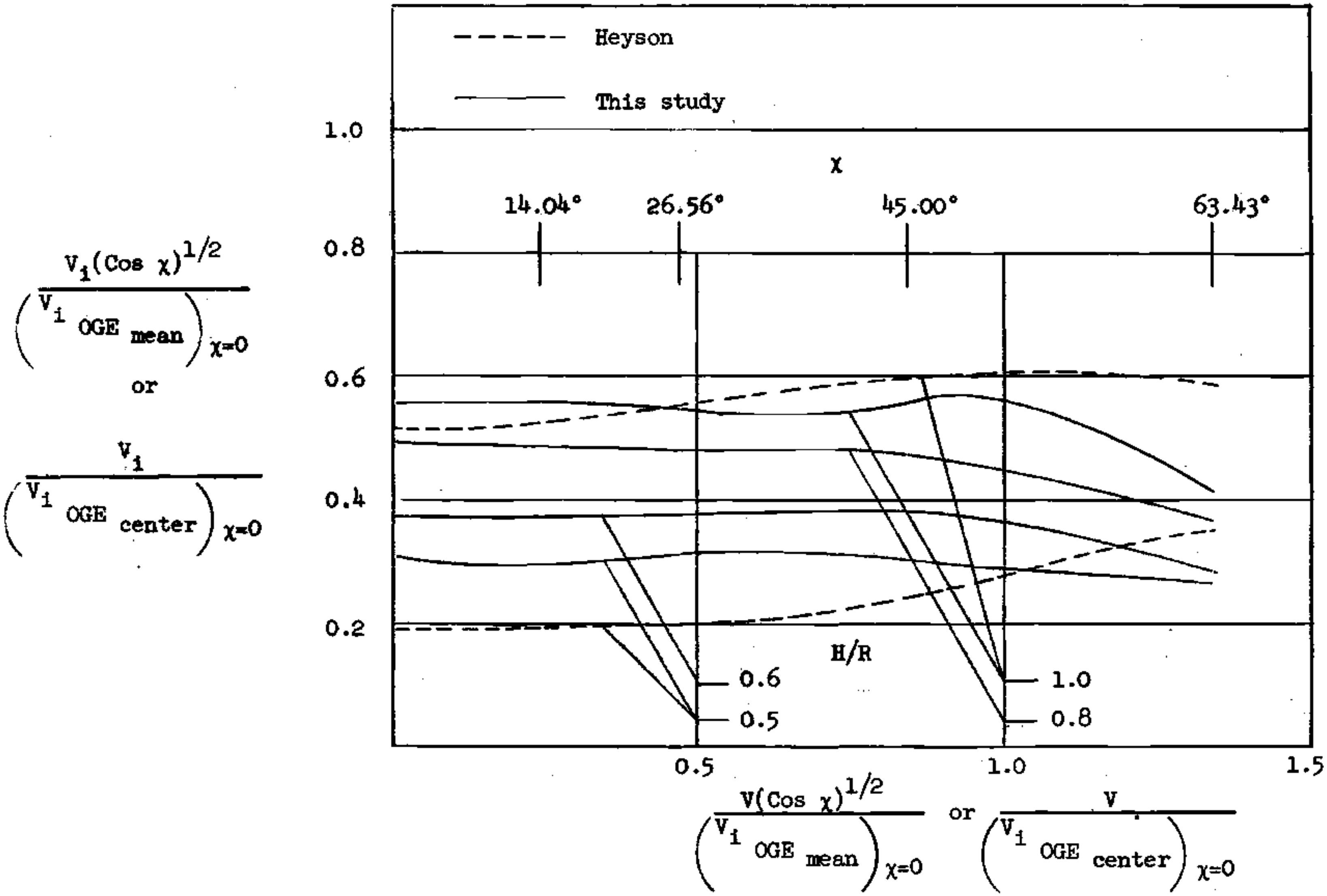

Figure 14. Induced Velocity Variation with Forward Flight Near the Ground--Uniform Disk Loading

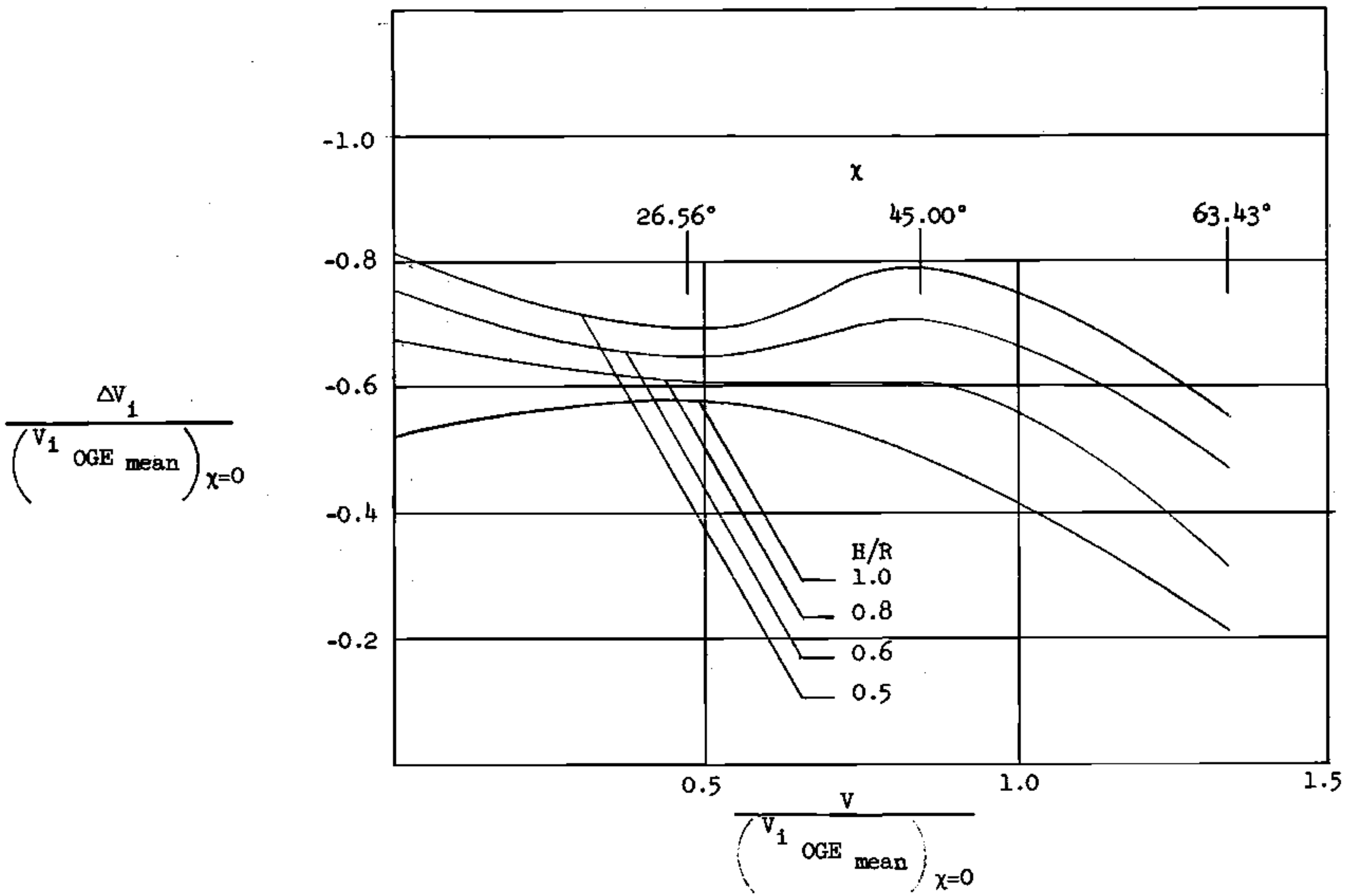

Figure 15. Variation of Ground-induced Interference Velocity with Forward Speed--Triangular Disk Loading

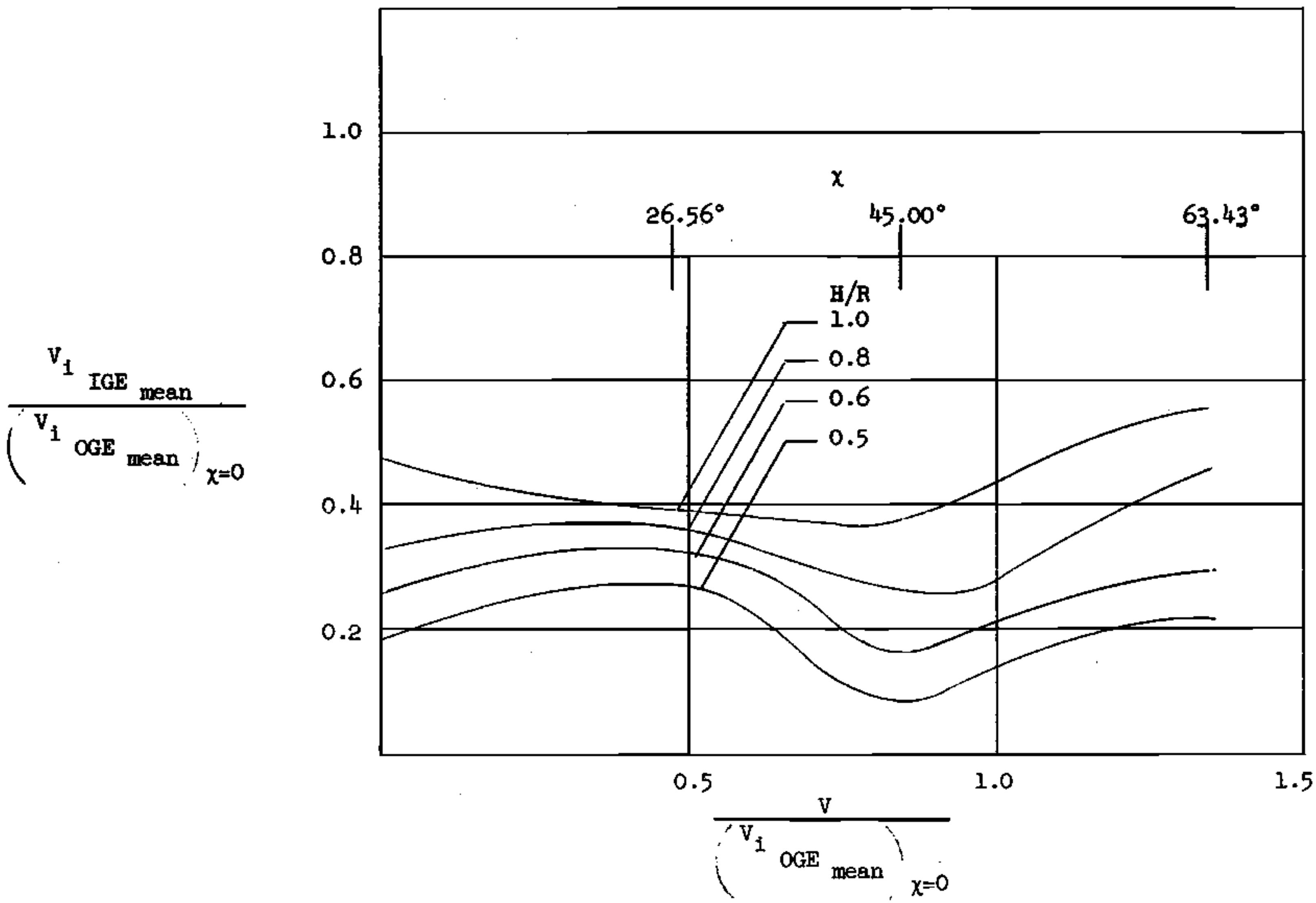

Figure 16. Variation of Mean Induced Velocity with Forward Speed--Triangular Disk Loading

BIBLIOGRAPHY

1. Heyson, Harry H., Ground Effect for Lifting Rotors in Forward Flight, National Aeronautics and Space Administration, Technical Note D-234, May 1960.

2. Castles, Walter, Jr., and De Leeuw, Jacob Henri, The Normal Component of the Induced Velocity in the Vicinity of a Lifting Rotor and Some Examples of its Application, National Advisory Committee for Aeronautics, Report 1184, 1954.

3. Heyson, Harry H., and Katzoff, S., Normal Component of Induced Velocity in the Vicinity of a Lifting Rotor with a Non-Uniform Disk Loading, National Advisory Committee for Aeronautics, Technical Note 3690, April 1956.

4. Knight, Montgomery, and Hefner, Ralph A., Analysis of Ground Effect on the Lifting Airscrew, National Advisory Committee for Aeronautics, Technical Note 835, December 1941.

5. Castles, Walter, Jr., and Durham, Howard L., Jr., Distribution of Normal Component of Induced Velocity in Lateral Plane of a Lifting Rotor, National Advisory Committee for Aeronautics, Technical Note 3841, December 1956.

6. Castles, Walter, Jr., Helicopter Performance Estimation, Unpublished Class Notes, Georgia Institute of Technology, 1959.